l./mol for the high $TeCl_4$ formality (0.161 *F*) using the best g_{II} value (0.24) and 24 ± 5 l./mol for the low $TeCl_4$ formality (0.064 *F*) using the best g_{II} value of 0.28.

Spectrum of Te_2^{2+}.—From three spectra of mixtures containing Te^{IV}, Te^{II}, and Te_2^{2+}, from the obtained values of g_I and g_{II}, and from the formalities of the tellurium and $TeCl_4$ added originally it is possible to calculate a spectrum of Te_2^{2+}. Such calculated spectra are shown in Figure 5. To obtain the ultraviolet part of the spectra a small path length (0.00836 cm) was used. Since the value of g_{II} is not well determined, three different g_{II} values, 0.25, 0.26, and 0.27, were used. A g_{II} value of 0.25 gives an α value close to 3, but a g_{II} value of 0.27 agrees better (as Table Ib shows) with the criteria of the best straight line. As the figure shows the formal absorptivity is not well defined, but at least an idea of the features of the spectrum can be obtained. Apparently only one broad band is present, located at *ca.* 29.3 kK. In order to obtain the molar absorptivity of Te_2^{2+} in Figure 5 the formal absorptivity should be multiplied by $^3/_2$, as is seen from the reaction $3Te^0 + Te^{IV} \rightarrow 2Te_2^{2+}$.

Acknowledgment.—The author wishes to thank P. Bødker for experimental assistance, M. Roy for programming, and the Northern Europe University Computing Center (NEUCC) for computing time.

CONTRIBUTION FROM THE DEPARTMENT OF CHEMISTRY,
MASSACHUSETTS INSTITUTE OF TECHNOLOGY, CAMBRIDGE, MASSACHUSETTS 02139

Three-Dimensional Macrocyclic Encapsulation Reactions. III.[1,2] Geometrical and Electronic Features of Tris(diimine) Complexes of Trigonal-Prismatic, Antiprismatic, and Intermediate Stereochemistry

BY E. LARSEN,[3] G. N. LA MAR, B. E. WAGNER, J. E. PARKS, AND R. H. HOLM*

Received April 4, 1972

The electronic properties of the generalized tris chelate $M(L-L)_3$, whose structure may be described in part by a twist angle ϕ, have been investigated over the trigonal-prismatic (TP, $\phi = 0°$) to trigonal-antiprismatic (TAP, $\phi = 60°$) range by the angular overlap method. One-electron d-orbital energies have been calculated as a function of angular parameters and energy-level schemes for TP $d^{7,8}$ and TP-TAP d^8 computed. Certain relationships between the twist angle and structural parameters of the coordination sphere have been derived. These considerations have been applied to the series of complexes $[M(PccBF)]^+$ (**1**), $[M((py)_3tach)]^{2+}$ (**2**), $[M((py)_3tame)]^{2+}$ (**3**), $[M((py)_3tren)]^{2+}$ (**4**), $[M(P(py)_3)_2]^{2+}$ (**7**), and $[M(bipy)_3]^{2+}$. X-Ray structural results have shown that these series encompass the TP and TAP structural extremes and include cases of intermediate stereochemistry. For the Fe(II), Co(II), Ni(II), and Zn(II) clathro chelates **1**, whose synthesis was reported in earlier parts of this series, the rigid ligand structure imposes smaller twist angles than for other complexes of these ions. The observed structural trends within the series **1**–**4** having constant ligand structure and variant metal ion may be rationalized in terms of destabilization of d^{6-8} configuration in TP compared to TAP geometry, with low-spin Fe(II) the most unstable (in agreement with earlier ligand-field calculations), and displacement toward the TAP geometry with decreasing ionic radius, other structural factors being approximately constant. Electronic spectra [Co(II), Ni(II)], pmr spectra [Ni(II)], polarographic redox potentials [Co(II), Fe(II)], and Mössbauer spectra [Fe(II)] of the above series of complexes have been found to undergo progressive, although not necessarily monotonic, changes with twist angle. Proton line widths of Ni(II) complexes have been observed to be particularly sensitive to stereochemistry and a qualitative model has been proposed. These results have been applied to the new sexadentate complexes of unknown stereochemistry $[M(P(CH_3pox)_3)]^{2+}$ (**5**) and $[M(P(bipy)_3)]^{2+}$ (**6**) [M = Fe(II), Co(II), Ni(II)], similar properties of which have been measured. The Ni(II) and Co(II) complexes are proposed to have intermediate solution stereochemistry, with that of the latter nearer the TP limit. The Fe(II) complexes are estimated to approach or perhaps achieve TAP geometry in solution and in the solid state.

Introduction

A rapidly accumulating body of evidence reveals that six-coordinate chelate complexes of the transition elements can adopt stable structures in which the $M-L_6$ coordination unit is significantly distorted from the usual octahedral or trigonal-antiprismatic (TAP, D_{3d}) microsymmetry while retaining a true or "pseudo" threefold rotation axis. Such structures may be partially described (*vide infra*) by a torsional or "twist" angle ϕ of the two L_3 donor atom triangles whose planes are normal to the threefold axis. Limiting values of ϕ are 60 and 0° for TAP and trigonal prismatic (TP) structures, respectively. X-Ray structural studies on complexes containing bidentate ligands have established TP coordination for certain oxidized metal tris(dithiolenes)[4] and tris(selenetenes),[5] $Er(dpm)_3$,[6a] and for the $Co-O_6$ unit in one diastereomer of $[Co(Co(OCH_2CH_2NH_2)_3)_2]^{2+}$.[6b] Intermediate geometries have been demonstrated recently for a number of tris-chelate species derived from anionic ligands such as tropolo-

---

[1] Part I: J. E. Parks, B. E. Wagner, and R. H. Holm, *J. Amer. Chem. Soc.*, **92**, 3500 (1970).

[2] Part II: J. E. Parks, B. E. Wagner, and R. H. Holm, *Inorg. Chem.*, **10**, 2472 (1971).

[3] NATO Postdoctoral Fellow, 1970–1971.

[4] R. Eisenberg, *Progr. Inorg. Chem.*, **12**, 295 (1970).

[5] C. G. Pierpont and R. Eisenberg, *J. Chem. Soc. A*, 2285 (1971).

[6] (a) J. P. R. de Villiers and J. C. A. Boeyens, *Acta Crystallogr., Sect. B*, **28**, 2335 (1971); (b) J. A. Bertrand, J. A. Kelly, and E. G. Vassian, *J. Amer. Chem. Soc.*, **91**, 2394 (1969).

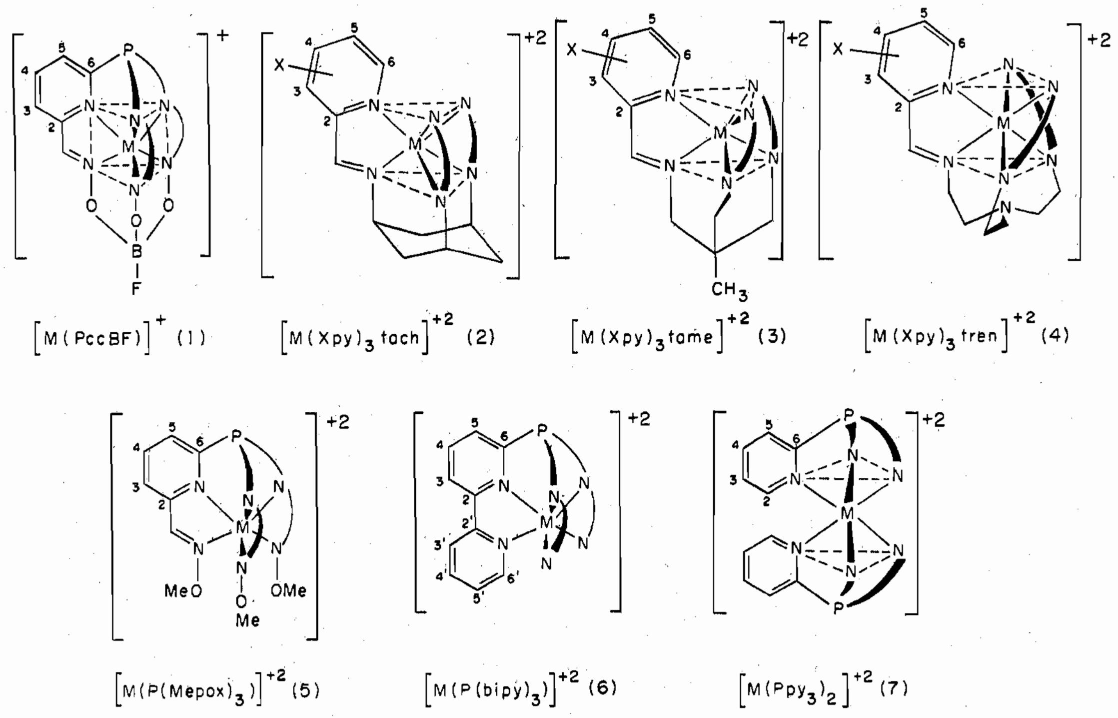

$[\mathrm{M(PccBF)}]^{+}$ (1) $[\mathrm{M(Xpy)_3tach}]^{+2}$ (2) $[\mathrm{M(Xpy)_3tame}]^{+2}$ (3) $[\mathrm{M(Xpy)_3tren}]^{+2}$ (4)

$[\mathrm{M(P(Mepox)_3)}]^{+2}$ (5) $[\mathrm{M(P(bipy)_3)}]^{+2}$ (6) $[\mathrm{M(Ppy_3)_2}]^{+2}$ (7)

Figure 1.—Schematic structural formulas for closed (**1**) and open (**2**–**6**) sexadentate and bis(tridentate) (**7**) metal(II) complexes. For purposes of clarity the detailed structure of only one chelate ring or a portion thereof is shown in each formula. The structures **1**–**4** are intended to indicate increasing departure from TP geometry usually found for a given M(II) (*cf.* Table I). No coordination geometries are implied by formulas **5** and **6**.

nate,[7a] N,N-disubstituted dithiocarbamates,[7b–f] and O-ethyl xanthate,[7g–i] whose relatively small bite distances (*ca.* 2.5–2.9 Å) appear to disallow octahedral coordination involving unexceptional M–L distances for certain metal ions. Such complexes are characterized by chelate ring bite angles (α) of *ca.* 73–78° and twist angles of 33–45°.

Results obtained in the last several years have clearly revealed that octahedral, TP, and intermediate geometries may be stabilized by the use of sexadentate ligands which contain a common binding group, pyridine-2-carboxaldimine, but differ in the extent of twist which occurs upon coordination to a given metal ion. Complexes of immediate pertinence are **1**–**4** (X = H), which are schematically depicted in Figure 1. Selected structural parameters are collected in Table I. The ligands involved are of two types. The complexes [M(PccBF)]$^+$ (**1**), whose preparation and characterization are reported in earlier parts[1,2] of this series, contain a bicyclic ligand which encapsulates the metal ion and forms a "clathro chelate"(cc).[8] Rigidity and dimensions of the ligand framework tend to stabilize TP geometry, as found for the Ni(II) complex,[9a] or to constrain an ion such as Fe(II), which is notably unstable in this geometry[10] (*vide infra*), from approaching closely octahedral coordination. The only other clathro chelates known, $[\mathrm{Co(dmg)_3(BF)_2}]^{0,1+}$,[11] possess structures which are nearly TP (Co(II), ϕ = 8.6°) or intermediate (Co(III), 22°).[12]

The remaining complexes, $[\mathrm{M((py)_3tach)}]^{2+}$ (**2**), $[\mathrm{M((py)_3tame)}]^{2+}$ (**3**), and $[\mathrm{M((py)_3tren)}]^{2+}$ (**4**), are formed by condensation of pyridine-2-carboxaldehyde with *cis,cis*-1,3,5-triaminocyclohexane, 1,1′,1′′-tris(aminomethyl)ethane, and 2,2′,2′′-triaminotriethylamine, respectively, in the presence, or shortly before the addition, of a metal(II) salt. The sexadentate ligands are of the open trifurcated type. As the data in Table I show, the presence of only one anchoring atom or group on the C_3 axes of the complexes together with more flexible connecting linkages (**3**, **4**) leads to less sterically constrained structures than is the case for the complexes **1**. For a given metal ion, the angle ϕ in **1** is substantially smaller than it is in **2**, **3**, and **4**.

$[\mathrm{M((py)_3tach)}]^{2+,3+}$ species were first prepared by Lions and Martin.[13] The possibility that structural constraints imposed by the ligand might lead to "unusual coordination geometries" was not recognized until somewhat later.[14] X-Ray results have now demonstrated that the Zn(II) complex very closely approaches TP geometry[15] and that the Ni(II) complex

---

(7) (a) T. A. Hamor and D. J. Watkin, *Chem. Commun.*, 440 (1969); (b) S. Merlino, *Acta Crystallogr., Sect. B*, **24**, 1441 (1968); (c) B. F. Hoskins and B. P. Kelly, *Chem. Commun.*, 1517 (1968); (d) A. Avdeef, J. P. Fackler, Jr., and R. G. Fischer, Jr., *J. Amer. Chem. Soc.*, **92**, 6972 (1970); (e) D. L. Johnston, W. L. Rohrbaugh, and W. D. Horrocks, Jr., *Inorg. Chem.*, **10**, 1474 (1971); (f) P. C. Healy and A. H. White, *Chem. Commun.*, 1446 (1971); (g) S. Merlino, *Acta Crystallogr., Sect. B*, **25**, 2270 (1969); (h) S. Merlino and F. Sartori, *ibid.*, **28**, 972 (1972); (i) B. F. Hoskins and B. P. Kelly, *Chem. Commun.*, 45 (1970); see also (j) E. I. Stiefel and G. F. Brown, *Inorg. Chem.*, **11**, 434 (1972).

(8) D. H. Busch, *Rec. Chem. Progr.*, **25**, 107 (1964).

(9) (a) M. R. Churchill and A. H. Reis, Jr., *Chem. Commun.*, 879 (1970); *Inorg. Chem.*, **11**, 1811 (1972); (b) M. R. Churchill and A. H. Reis, Jr., *Chem. Commun.*, 1307 (1971); *Inorg. Chem.*, in press; (c) M. R. Churchill and A. H. Reis, Jr., results to be published.

(10) W. O. Gillum, R. A. D. Wentworth, and R. F. Childers, *Inorg. Chem.*, **9**, 1825 (1970).

(11) (a) D. R. Boston and N. J. Rose, *J. Amer. Chem. Soc.*, **90**, 6859 (1968); (b) D. R. Boston and N. J. Rose, Abstracts, 157th National Meeting of the American Chemical Society, April 1969, No. INOR 96.

(12) G. A. Zakrewski, C. A. Ghilardi, and E. C. Lingafelter, *J. Amer. Chem. Soc.*, **93**, 4411 (1971).

(13) F. Lions and K. V. Martin, *ibid.*, **79**, 1572 (1957).

(14) J. E. Sarneski and F. L. Urbach, *Chem. Commun.*, 1025 (1968).

(15) W. O. Gillum, J. C. Huffman, W. E. Streib, and R. A. D. Wentworth, *ibid.*, 843 (1969).

TABLE I

SELECTED ANGULAR STRUCTURAL PARAMETERS FOR SEXADENTATE AND TRIS-CHELATE $M-N_6$ COMPLEXES IN THE SOLID STATE

Compound	Twist angle ϕ, deg	Bite angle α, deg	Ref
$[Fe(PccBF)](BF_4)^a$	21, 22, 22	78–79	9b
$[Co(PccBF)](BF_4)^k$	0.4, 1.0, 3.2	74–76	9c
$[Ni(PccBF)](BF_4)$	1.1, 1.8, 1.8	76–78	9a
$[Zn(PccBF)](BF_4)$	1.1, 2.3, 2.3	76–81	9c
$[Ni((py)_3tach)](ClO_4)_2$	30, 33, 34	77–80	*m*
$[Zn((py)_3tach)](ClO_4)_2{}^b$	2.0, 5.0, 6.6	74	*n*
$[Fe((py)_3tame)](ClO_4)_2$	39, 45, 45	80–81	19b
$[Zn((py)_3tame)](ClO_4)_2{}^c$	28^h	76–77	19a
$[Fe((py)_3tren)](BF_4)_2$	54^h	81	*o, p*
$[Co((py)_3tren)]^{2+\,d}$	49^h	76	*p*
$[Ni((py)_3tren)](PF_6)_2$	51^h	78	*p*
$[Zn((py)_3tren)]^{2+\,d}$	46^h	76	*p*
$[Fe(phen)_3]$(antimonyl *d*-tartrate)$_2$	$\sim 56^{h,i}$	83^i	*e*
$K[Ni(phen)_3][Co(C_2O_4)_3]$		80	*f*
$[Ni(phen)_3][S_2P(OCH_3)_2]_2$	$\sim 50^{h,j}$	80^j	*g*
$[Ni(phen)_3][Mn(CO)_5]_2$		79	*l*

[a] Dichloromethane solvate. [b] Co(II) complex isomorphous. [c] Co(II), Ni(II) complexes isomorphous. [d] Anion unspecified. [e] D. H. Templeton, A. Zalkin, and T. Ueki, *Acta Crystallogr., Sect. A*, **21**, 154 (1966). [f] K. R. Butler and M. R. Snow, *J. Chem. Soc. A*, 565 (1971). [g] M. Shiro and Q. Fernando, *Chem. Commun.*, 350 (1971). [h] Average value. [i] Calculated from data supplied by Professor D. Templeton and Dr. A. Zalkin. [j] Calculated from data supplied by Prof. Q. Fernando. [k] Acetonitrile solvate. [l] B. A. Frenz and J. A. Ibers, *Inorg. Chem.*, **11**, 1109 (1972). [m] E. B. Fleischer, A. E. Gebala, and D. R. Swift, *Chem. Commun.*, 1280 (1971). [n] W. O. Gillum, J. C. Huffman, W. E. Streib, and R. A. D. Wentworth, *ibid.*, 843 (1969). [o] C. Mealli and E. C. Lingafelter, *ibid.*, 885 (1970). [p] E. C. Lingafelter, private communication.

has an average twist angle of *ca.* 32°.[16] Synthesis and spectral properties of a series of $[M((py)_3tach)]^{2+}$ complexes have recently been described in some detail by Gillum, *et al.*[10] The first $[M((py)_3tame)]^{2+}$ species to be prepared was the Fe(II) complex,[17] although an earlier paper[18] had described the synthesis of the analogous complex in which the bridgehead methyl group was replaced by hydrogen. In neither report was the possibility of nonoctahedral coordination mentioned. Structural studies by Fleischer, *et al.*, have since demonstrated that the Zn(II)[19a] and Fe(II)[19b] complexes possess coordination geometries intermediate between the TP and TAP limits. The pmr spectra of both complexes[19a,20] imply that they retain chiral structures in solution. The complete series of $[M((py)_3tren)]^{2+}$ complexes, M = Mn(II)–Zn(II), has been prepared by Wilson and Rose.[21] The structures of all members of the series have been solved,[22] revealing that for complexes **1–4** with a given metal ion, $[M((py)_3tren)]^{2+}$ most closely approaches a TAP structure.

Because the complexes **1–4** effectively span the structural limits (TP, TAP) of six-coordination and include a number of examples of intermediate geometries, they constitute a unique structural series. Consequently, this series provides a previously unavailable opportunity to examine the effects of varying stereochemistry on the electronic properties of complexes containing a common coordinating group. Reported herein are the results of an investigation of the electronic and nmr spectra of complexes of this type. Some polarographic data are also reported. Nickel(II) and cobalt(II) complexes have been investigated in the most detail in order to ascertain if progressive structural change from TP to TAP is reflected in certain spectroscopic features, thereby leading to experimental stereochemical criteria. In addition the complexes **5** and **6** (Figure 1), derived from the new sexadentate ligands tris(2-*O*-methylcarboxaldoximo-6-pyridyl)phosphine and tris(6-(2,2′-bipyridyl))phosphine, respectively, have been prepared. Certain spectral features have been determined and compared with those of **1–4** in an attempt to deduce the stereochemistry of these complexes.

Experimental Section

Preparation of Compounds.—*cis,cis*-1,3,5-Triaminocyclohexane[23,24] (tach) and 1,1′,1″-tris(aminomethyl)ethane[23,25] (tame) were obtained by published procedures. 2,2′,2″-Triaminotriethylamine (tren) was prepared in 34% yield by the Hoffmann rearrangement of 3,3′,3″-nitrilotrispropionamide and was purified by distillation; bp 90–94° (0.5 mm). The method of Ginsberg and Wilson[26] was employed in the preparation of 3-, 4-, and 5-methylpyridine-2-carboxaldehydes. Analytical data for new complexes are given in Table II.

(a) ***cis,cis*-1,3,5-Tris(pyridine-2-carboxaldimino)cyclohexanemetal(II) Perchlorates, $[M((Xpy)_3tach)](ClO_4)_2$ (2, X = H, 3-CH_3, 4-CH_3, 5-CH_3).**—Unsubstituted complexes with M = Fe(II), Co(II), Ni(II) were prepared by published methods.[10,13]

$[Ni((4\text{-}CH_3py)_3tach)](ClO_4)_2$.—The *cis,cis*-triamine (0.13 g, 1.0 mmol), 0.36 g (3.0 mmol) of 4-methylpyridine-2-carboxaldehyde and 0.24 g (1.0 mmol) of nickel chloride hexahydrate were refluxed in 30 ml of ethanol for 1 hr. The red solution was reduced in volume and the red complex precipitated by the addition of 40 ml of a saturated solution of sodium perchlorate in ethanol. The product was collected by filtration, washed with cold water, and recrystallized twice from boiling water to yield 0.28 g (40%) of dark red needles; ν_{CN} 1645 cm^{-1} (mull).

$[Ni((3\text{-}CH_3py)_3tach)](ClO_4)_2$.—This compound was prepared by the above procedure employing 3-methylpyridine-2-carboxaldehyde, but was recrystallized from acetonitrile. Pale red crystals were obtained in 65% yield; ν_{CN} 1645 cm^{-1} (mull).

$[Ni((5\text{-}CH_3py)_3tach)](ClO_4)_2$.—This compound was obtained from 5-methylpyridine-2-carboxaldehyde following the published procedure.[10] The product was recrystallized from cold aqueous ethanol and isolated in 28% yield as a dark red powder. It was not analyzed but was identified by its pmr spectrum (acetone-d_6, 29°; 3-H, −50.1; 4-H, −14.1; 5-CH_3, +3.8; cyclohexyl, +4.5, +8.6 ppm) and infrared spectrum (mull, ν_{CN} 1645 cm^{-1}).

(b) **1,1′,1″-Tris(pyridine-2-carboxaldimino)ethanemetal(II) Perchlorates, $[M((Xpy)_3tame)](ClO_4)_2$ (3, X = H, 3-CH_3, 4-CH_3).**—The series of unsubstituted complexes with M = Mn(II)–Zn(II) (excluding Cu(II)) has been reported. The Fe(II), Co(II), and Ni(II) complexes were prepared by the method briefly described[19a] and their purities established by elemental analyses.

---

[16] E. B. Fleischer, A. E. Gebala, and D. R. Swift, *Chem. Commun.*, 1280 (1971).

[17] D. A. Durham, F. A. Hart, and D. Shaw, *J. Inorg. Nucl. Chem.*, **29**, 509 (1967).

[18] F. P. Dwyer, N. S. Gill, E. C. Gyarfas, and F. Lions, *J. Amer. Chem. Soc.*, **79**, 1269 (1957).

[19] (a) E. B. Fleischer, A. E. Gebala, and P. Tasker, *ibid.*, **92**, 6365 (1970); (b) E. B. Fleischer, A. E. Gebala, D. R. Swift, and P. A. Tasker, *Inorg. Chem.*, **11**, 2775 (1972).

[20] L. F. Urbach and S. O. Wandiga, *Chem. Commun.*, 1572 (1970). For a recent study of $[M((py)_3tame)]^{2+,3+}$ complexes see S. O. Wandiga, J. E. Sarneski, and F. L. Urbach, *Inorg. Chem.*, **11**, 1349 (1972).

[21] (a) L. J. Wilson and N. J. Rose, Abstracts, 158th National Meeting of the American Chemical Society, Sept 1969, No. INOR 89; N. J. Rose, private communication; (b) L. J. Wilson and N. J. Rose, *J. Amer. Chem. Soc.*, **90**, 6041 (1968).

[22] (a) C. Mealli and E. C. Lingafelter, *Chem. Commun.*, 885 (1970); (b) E. C. Lingafelter, private communication.

[23] E. B. Fleischer, A. E. Gebala, A. Levey, and P. A. Tasker, *J. Org. Chem.*, **36**, 3042 (1971).

[24] R. A. D. Wentworth and J. J. Felton, *J. Amer. Chem. Soc.*, **90**, 621 (1968).

[25] H. Stetter and W. Böckman, *Chem. Ber.*, **84**, 834 (1951).

[26] S. Ginsberg and I. B. Wilson, *J. Amer Chem. Soc.*, **79**, 481 (1957).

TABLE II

CHARACTERIZATION DATA FOR M–N_6 COMPLEXES

Compound	Color	% calcd			% found		
		C	H	N	C	H	N
$[Ni((4-CH_3py)_3tach)](ClO_4)_2$	Dark red	46.58	4.34	12.07	46.35	4.34	11.82
$[Ni((3-CH_3py)_3tach)](ClO_4)_2$	Pale red	46.58	4.34	12.07	46.15	4.31	12.00
$[Ni((4-CH_3py)_3tame)](ClO_4)_2$	Red-brown	45.64	4.42	12.28	45.58	4.54	12.52
$[Ni((3-CH_3py)_3tame)](ClO_4)_2$	Yellow	45.64	4.42	12.28	46.01	4.50	12.53
$[Ni((4-CH_3py)_3tren)](ClO_4)_2$	Yellow-brown	45.47	4.66	13.75	45.15	4.67	13.53
$[Ni((3-CH_3py)_3tren)](ClO_4)_2$	Yellow	45.47	4.66	13.75	45.38	4.46	13.29
$[Fe(P(CH_3pox)_3)](ClO_4)_2$	Red-purple	36.49	3.06	12.15	36.66	3.10	12.15
$[Co(P(CH_3pox)_3)](BF_4)_2$	Yellow	37.70	3.16	12.56	37.17	3.12	12.09
$[Ni(P(CH_3pox)_3)](ClO_4)_2$[a]	Light brown	37.38	3.35	11.61	37.61	3.40	11.55
$[Fe(P(bipy)_3)](ClO_4)_2$	Red-black	47.96	2.82	11.19	47.91	2.83	11.22
$[Co(P(bipy)_3)](ClO_4)_2$	Yellow	47.76	2.81	11.14	47.76	2.84	11.14
$[Ni(P(bipy)_3)](ClO_4)_2$	Beige	47.78	2.81	11.14	47.74	2.74	11.19
$[Cu(P(bipy)_3)](ClO_4)_2$	Blue	47.48	2.77	11.07	47.66	3.03	11.07
$[Fe(P(py)_3)_2](ClO_4)_2$	Maroon	45.89	3.09	10.70	45.85	3.07	10.60
$[Co(P(py)_3)_2](ClO_4)_2$	Red-brown	45.71	3.07	10.66	45.77	3.07	10.67
$[Ni(P(py)_3)_2](ClO_4)_2$	Pale violet	45.72	3.07	10.66	45.92	3.13	10.59
$[Cu(P(py)_3)_2](ClO_4)_2$	Light blue	45.44	3.05	10.59	45.08	3.30	11.49
$[Ni(4-CH_3PccBF)](BF_4)$	Golden	41.43	2.98	13.81	41.72	3.05	13.80

[a] Acetone hemisolvate.

$[Ni((3-CH_3py)_3tame)](ClO_4)_2$.—The triamine (2.0 mmol), 6.0 mmol of 3-methylpyridine-2-carboxaldehyde, and 2.0 mmol of nickel chloride hexahydrate were refluxed in 30 ml of ethanol for 8 hr. To the reaction mixture was added 40 ml of a saturated solution of sodium perchlorate in ethanol. The red precipitate was collected, washed with water and ethanol, and recrystallized from acetonitrile. The compound was obtained as a yellow solid (73%); ν_{CN} 1645 cm^{-1} (mull).

$[Ni((4-CH_3py)_3tame)](ClO_4)_2$.—The preceding preparation was employed with 4-methylpyridine-2-carboxaldehyde. Red-brown crystals (58%) were obtained from acetonitrile; ν_{CN} 1645 cm^{-1} (mull).

(c) **3,3′,3′′-Tris(pyridine-2-carboxaldimino)nitrilotriethane-metal(II) Perchlorates, $[M((Xpy)_3tren)](ClO_4)_2$ (4, X = H, 3-CH_3, 4-CH_3).**—$[Ni((py)_3tren)](ClO_4)_2$ was obtained by a procedure described for other salts of the same cation.[21b] The Co(II) and Fe(II) salts were prepared by the same method and their purities established by elemental analyses.

$[Ni((3-CH_3py)_3tren)](ClO_4)_2$.—The triamine (2.0 mmol), 6.0 mmol of 3-methylpyridine-2-carboxaldehyde, and 2.0 mmol of nickel chloride hexahydrate were refluxed in 50 ml of ethanol for 8 hr. Volume reduction of the dark red solution and addition of 2 g of sodium perchlorate gave a yellow solid. Recrystallization from acetonitrile afforded a yellow solid (70%); ν_{CN} 1640 cm^{-1} (mull).

$[Ni((4-CH_3py)_3tren)](ClO_4)_2$.—The preceding method was used with 4-methylpyridine-2-carboxaldehyde. The product was recrystallized from acetone and obtained as a yellow powder (31%); ν_{CN} 1640 cm^{-1} (mull).

(d) **Tris(2-*O*-methylcarboxaldoximo-6-pyridyl)phosphine, $P(CH_3pox)_3$, and Its Metal(II) Complexes, $[M(P(CH_3pox)_3)]^{2+}$ (5). $P(CH_3pox)_3$.**—Tris(2-(1,3-dioxolan-2-yl)-6-pyridyl)phosphine[2] (5.25 g, 11.0 mmol) was suspended in 100 ml of degassed water at 50°, and 7.5 ml of concentrated hydrochloric acid and 4.2 g (50 mmol) of *O*-methylhydroxylamine hydrochloride were added. A yellow-orange precipitate formed after stirring for 2 hr. The suspension was cooled in an ice bath, treated dropwise with aqueous sodium hydroxide solution until neutral, and filtered. The crude product was washed with water and recrystallized twice from ethanol. After drying *in vacuo* for 6 hr 3.5 g (82%) of colorless crystals was obtained, mp 101–102°. Pmr ($CDCl_3$): -3.74 (singlet, 3, CH_3), -7.1 to -7.8 (multiplet, 3, ring H), -7.98 (singlet, 1, HC=N). *Anal.* Calcd for $C_{21}H_{21}N_6O_3P$: C, 57.80; H, 4.85; N, 19.25. Found: C, 57.84; H, 5.06; N, 18.94.

$[Fe(P(CH_3pox)_3)](ClO_4)_2$.—Filtered solutions of ferrous perchlorate hexahydrate (0.36 g, 1 mmol) in 20 ml of ethanol and $P(CH_3pox)_3$ (0.44 g, 1 mmol) in 30 ml of hot ethanol were mixed, stirred for 5 min, and cooled. The red-purple crystals obtained were recrystallized from acetonitrile–ethanol to afford 0.50 g (72%) of pure product. The compound is diamagnetic in the solid state.

$[Co(P(CH_3pox)_3)](BF_4)_2$.—Filtered degassed solutions of cobaltous tetrafluoroborate hexahydrate (0.34 g, 1.0 mmol) in 20 ml of acetonitrile and $P(CH_3pox)_3$ (0.44 g, 1.0 mmol) in 10 ml of acetonitrile were mixed and stirred for 5 min. Reduction in volume and addition of acetone precipitated yellow needles. After drying *in vacuo* for 8 hr at 100° 0.50 g (74%) of product was obtained.

$[Ni(P(CH_3pox)_3)](ClO_4)_2$.—This compound was prepared analogously to the cobalt(II) complex and obtained in the form of an acetone hemisolvate as light brown needles (0.45 g, 62%).

(e) **Tris(6-(2,2′-bipyridyl))phosphine, $P(bipy)_3$, and Its Metal(II) Complexes, $[M(P(bipy)_3)](ClO_4)_2$ (6). $P(bipy)_3$.**—Under a nitrogen atmosphere a solution of 7.05 g (30 mmol) of 6-bromo-2,2′-bipyridyl[27] in 30 ml of dry diethyl ether was added over 3 min to a solution of 18.5 ml of 1.6 *N* *n*-butyllithium (30 mmol) in 50 ml of diethyl ether which had been previously cooled to $-100°$ in a pentane slush bath. The temperature of the dark reddish violet solution rose briefly to $-60°$ and then was maintained at $-80°$ for 45 min. At this point a solution of 1.38 g (10 mmol) of freshly distilled phosphorus trichloride in 25 ml of dry ether was added during 25 min. The pale orange suspension was vigorously stirred for 1 hr at $-80°$ and then allowed to warm to $-30°$ over the course of about 4 hr. Methanol (10 ml) was introduced to discharge any unreacted organolithium species, 50 ml of water was added, ether removed on a rotary evaporator, and the resultant mixture extracted with 75 ml of chloroform. The extract was washed with 50 ml of water, dried (sodium sulfate), and evaporated to yield a brown oil. The oil was dissolved in the minimum volume of benzene and chromatographed with benzene on alumina (Woelm, Activity Grade III, 300 × 35 mm column). The first 450 ml of eluate contained 2,2′-bipyridyl, 6-bromo-2,2′-bipyridyl, and a yellow oil (1.6 g total). The next 500 ml contained all of the desired product; 1.1 g of crude material was obtained upon removal of solvent. This was recrystallized from chloroform–methanol (two crops taken) and then from benzene–hexane to afford 0.71 g (17%) of white crystals, mp 178.5–180.5° (cor). The mass spectrum (70 eV) displayed the parent ion peak at *m/e* 496. *Anal.* Calcd for $C_{30}H_{21}N_6P$: C, 72.57; H, 4.26; N, 16.93. Found: C, 71.76; H, 4.00; N, 16.92.

$[M(P(bipy)_3)](ClO_4)_2$, M = Fe(II), Co(II), Ni(II), Cu(II).—The complexes were prepared by mixing filtered solutions of 0.25 g (0.50 mmol) of $P(bipy)_3$ in 20 ml of acetone and 0.50 mmol of the metal(II) perchlorate hexahydrate in 10 ml of acetone. The solutions (Fe(II), deep red; Co(II), yellow; Ni(II), red-brown; Cu(II), blue-green) were reduced in volume until crystallization commenced, cooled, and filtered. The complexes were recrystallized from acetonitrile–ethanol to give nicely crystalline solids: Fe(II), red-black needles, 0.28 g (76%); Co(II), fine yellow plates or needles, 0.17 g (46%); Ni(II), beige needles, 0.25 g (67%); Cu(II), blue needles, 0.25 g (66%).

(f) **Bis(tri-2-pyridylphosphine)metal(II) Perchlorates,[28] [M-**

---

(27) F. H. Burstall, *J. Chem. Soc.*, 1662 (1938).

(28) Note that the numbering scheme used for **7** in Figure 1 is consistent with that for other complexes and does not correspond to correct ligand nomenclature.

$(P(py)_3)_2](ClO_4)_2$ (7).—Contrary to a recent report[29] a previously published method[30] for the preparation of tri-2-pyridylphosphine, involving transmetalation of 2-bromopyridine with *n*-butyllithium followed by reaction with phosphorus trichloride, was found to be repeatable. The pure compound was obtained in 35% yield. Complexes of Fe(II), Ni(II), and Cu(II) were prepared by mixing warm filtered solutions of 1 mmol of the metal(II) perchlorate hexahydrate in 10 ml of acetone and 3 mmol of the ligand in 10 ml of acetone and reducing the volume of the resulting solutions where necessary to initiate crystallization. The compounds were recrystallized from acetonitrile and were obtained in *ca.* 70% yield. The Co(II) complex was prepared using degassed solutions and was recrystallized from boiling oxygen-free ethanol; a 70% yield was obtained.

(g) **Fluoroborotris(2-carboxaldoximo-6-pyridyl)phosphinemetal(II) Tetrafluoroborates, $[M(PccBF)](BF_4)$ (1).**—Complexes with M = Fe(II), Co(II), Ni(II), and Zn(II) were synthesized by the methods described recently.[1,2]

$[Ni(4\text{-}MePccBF)](BF_4)$.—Previously reported methods[31] were used to prepare diethyl α-cyano-β-methylglutaconate and to convert it, *via* 4-methyl-2,6-dihydroxypyridine, to 4-methyl-2,6-dibromopyridine. Tris(6-carboxaldoximo-4-methyl-2-pyridyl)phosphine was obtained in low yield from the latter compound and was converted to the Ni(II) clathro chelate by reactions analogous to those described elsewhere.[1,2,32] The complex tetrafluoroborate salt was purified by chromatography on alumina with acetonitrile followed by recrystallization from acetonitrile–ethanol.

Electronic Spectra.—All solution and crystal spectra were measured at ambient temperature using a Cary Model 14 spectrophotometer. The spectrum of [Co(PccBF)] was obtained by controlled potential electrolysis of an acetonitrile solution of $[Co(PccBF)](BF_4)$ employing a PAR Model 170 electrochemistry system as the potential source. The polarized crystal spectra of $[Co(PccBF)](BF_4)$ (pure crystal) and $[Ni(PccBF)](BF_4)$ (diluted in crystals of the Zn(II) analog) were determined in the near-infrared region. Pure crystals of the three compounds are isomorphous[9] and contain four cations in the monoclinic unit oriented such that their pseudo-C_3 axes (*cf.* Table I) are parallel and parallel to the vector bisecting the β angle. From precession photographs it was ascertained that the direction of propagation of light along the short crystal edge was parallel to the crystallographic twofold axis. The angle was also found between the two long edges. Axial and perpendicular spectra were obtained by allowing the plane of polarization to bisect the 108° angle between the crystal edges or to be normal to this direction, respectively. A Polaroid HR linearly polarizing ir filter was used as the polarizer, and neutral density screens were placed in the reference beam of the spectrophotometer. The absorption feature in the 8000–12,000 cm^{-1} region of the Ni(II) complex was found to be almost entirely polarized perpendicular to the pseudo-threefold axis. The band at 8100 cm^{-1} in the Co(II) complex did not show a pronounced polarization in either direction, nor did the shoulder at $\sim$20,500 cm^{-1} in the Ni(II) complex.

Other Physical Measurements.—Magnetic moments in the solid state were determined by the Faraday method using $HgCo(NCS)_4$ as the calibrant. Proton nmr spectra were recorded on a Varian HA-100 spectrometer operating in the HR mode modified for variable frequency modulation. Peak calibrations were made by the usual audio-side-band technique. Line widths quoted in Table IV are defined as full width at half-height under nonsaturation conditions and are reported in Hz at 100 MHz. Temperatures at other than ambient temperature ($\sim$29°) were regulated with a Varian V-4343 temperature control unit which was precalibrated with methanol and ethylene glycol. Polarographic measurements were made on acetonitrile solutions at 25° with a Princeton Applied Research Model 170 electrochemistry system or an ONRL Model 1988 polarograph. The working electrode was either a dropping mercury or rotating platinum electrode and the supporting electrolyte was 0.05 *M* tetra-*n*-propylammonium perchlorate. Potentials were measured *vs.* sce.

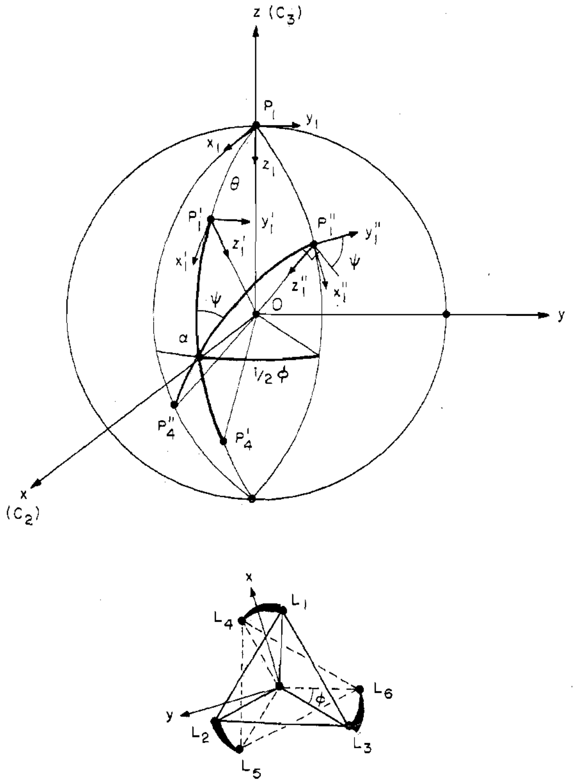

Figure 2.—Top: coordinate system used in angular overlap calculations, illustrating the bite angle α (P_1'–P_4' and P_1''–P_4''), the tilt angle ψ, and the twist angle φ. The points P_1', P_4' and P_1'', P_4'' represent the positions of the ligand atoms L_1 and L_4 on the spherical surface in TP geometry (φ = 0°) and after rotation about the C_2 axis. Bottom: illustration of the twist angle in terms of a projection of metal–ligand vectors in the *xy* plane.

Results and Discussion

Stereochemical and Electronic Considerations.—In examining the stereochemical and certain electronic features of unsaturated chelate complexes having coordination geometries ranging from TP to TAP, the generalized complex $M(L\text{–}L)_3$ with idealized structural features is first considered. This complex possesses D_{3h} symmetry in the TP configuration and D_3 symmetry in all other configurations of interest and contains ligands with out-of-plane π orbitals designated as π^s. Its geometry may be described by the orthogonal coordinate system of Figure 2, which is equivalent to that used by Schäffer[33] in his treatment of the angular overlap model (AOM). The metal is at the origin, the *z* axis is the trigonal axis, and the *x* axis is a twofold symmetry axis. For chelate L_1–L_4 shown in the figure the ligand atoms have the general angular coordinates θ, $\phi/2$, $\psi(L_1)$ and $\pi - \theta$, $-\phi/2$, $\psi(L_4)$. The bite angle $\alpha = L_1OL_4$ and is defined by $d = 2r \sin \alpha/2$, where *d* is the bite distance and *r* the M–L distance. In the TP arrangement L_1 and L_4 are located at points P_1' and P_4' on the sphere and the coordinates of L_1 are $\pi/2 - \alpha/2$, 0, 0. Nonprismatic geometry may be generated by rotation of each chelate by an equal amount in the same sense around its twofold axis, placing, *e.g.*, L_1 at P_1'' and L_4 at P_4'' and resulting in simultaneous

---

[29] H. J. Jakobsen, *J. Mol. Spectrosc.*, **34**, 245 (1970).

[30] E. Płażek and R. Tyka, *Zesz. Nauk. Politech. Wroclaw., Chem.*, **No. 4**, 79 (1957); *Chem. Abstr.*, **52**, 20156*c* (1958).

[31] G. A. R. Kon and H. R. Nangi, *J. Chem. Soc.*, 560 (1931); D. E. Ames, R. E. Bowman, and T. F. Grey, *ibid.*, 3008 (1953); H. Rogerson and J. F. Thorpe, *ibid.*, **87**, 1689 (1905); D. E. Ames and T. F. Grey, *ibid.*, 631 (1951).

[32] New intermediate compounds were not analyzed but were identified by pmr and infrared spectra.

[33] C. E. Schäffer, *Struct. Bonding* (*Berlin*), **5**, 68 (1968).

changes in the angles θ, ϕ, and ψ. The latter describes the angle of tilt between the chelate-ring plane and the trigonal axis.[34] From spherical geometry it follows that the coordinates of L_1 are related by the expressions

$$\cos \alpha/2 = \sin \theta \cos \phi/2 \qquad (1)$$

$$\sin \alpha/2 = \cos \theta/\cos \psi \qquad (2)$$

The angle ϕ, referred to as the twist angle, is defined by the projection of metal–ligand vectors of a chelate ring on the *xy* plane (*cf.* Figure 2). With a constant bite angle of, *e.g.*, 77°, the polar angle θ changes from 51.5 to 64.6° and the tilt angle ψ from 0 to 46.5° upon passing from the prism ($\phi = 0°$) to the antiprism ($\phi = 60°$). For complexes with trigonal microsymmetry or for those which possess the minimal feature of two parallel L_3 donor triangles centered on a normal passing through the metal, the twist angles are well defined structural parameters. The situation is rather closely approached by the majority of complexes in Table I, especially by the [M(PccBF)]$^+$ species. Among the more distorted complexes such as [Ni((py)$_3$tach)]$^{2+}$ [16] the twist angles listed are not as precisely defined. However, in all cases they are considered meaningful semiquantitative structural parameters and are employed in the discussions which follow. The angle ψ is a somewhat less useful parameter due to the lack of ligand planarity in a number of complexes.

Based on the twist angles in Table I for the complexes **1**–**4**, several structural trends may be recognized. Fe(II), Co(II), and Ni(II) complexes of these types have ground-state spins of 0, $^3/_2$, and 1, respectively. For complexes of a given metal ion the relative tendency of the ligands to approach TP coordination is

$$\text{PccBF} > (\text{py})_3\text{tach} \gtrsim (\text{py})_3\text{tame} > (\text{py})_3\text{tren} \qquad (3)$$

Variation of metal ion coordinated to a given ligand results in the series

$$\text{Zn(II)} \gtrsim \text{Co(II)} \gtrsim \text{Ni(II)} > \text{Fe(II)} \qquad (4)$$

Series 3 is quite well defined for the four Zn(II) complexes, in which metal ion directional effects are absent. The position of PccBF in this series is clearly due to its rigid bicyclic structure, which is significantly distorted from the TP configuration only by Fe(II). The series is also followed by three Fe(II) and Ni(II) complexes. However, if [Ni((py)$_3$tame)]$^{2+}$ is similar to its isomorphous Zn(II) analog, it would appear that it and [Ni((py)$_3$tach)]$^{2+}$ have roughly comparable geometries. Series 4 is less clearly defined than series 3 but the terminal position of Fe(II) is well established. The order of Zn(II) and Co(II)–Ni(II) appears reversed in the PccBF complexes but the difference of only 0.3–0.4° in average twist angles is too small to be significant. The principal importance of the Zn(II) structures is that they provide an indication of the closest approach to TP geometry possible for the ligands of series 3 when coordinated to a metal ion of the same charge and approximate size as Zn(II).

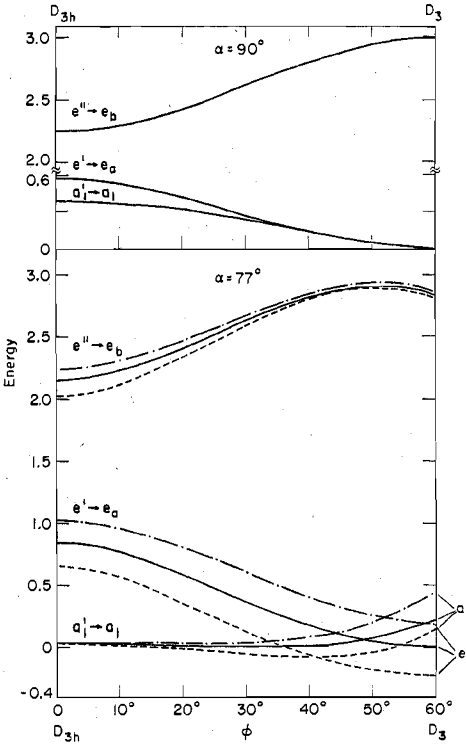

Figure 3.—Dependence of one-electron d-orbital energies (diagonalized) for the complex M(L–L)$_3$ (α = 77, 90°) upon the twist angle ϕ: ——, e_σ ($e_{\pi s} = 0$); –·–·, $e_{\pi s} = +0.1e_\sigma$; - - - -, $e_{\pi s} = -0.1e_\sigma$.

In considering the structural results summarized by series 3 and 4, it is pertinent to inquire what the geometry of certain metal(II) complexes might be in the absence of any steric constraints imposed by the sexadentate ligand structures. Restricting attention to complexes of the metal ions in series 4 with diimine-type ligands, crystallographic data adequate for this purpose are presently available only for [Fe(phen)$_3$]$^{2+}$ and [Ni(phen)$_3$]$^{2+}$ salts. Average twist and bite angles were calculated from atomic coordinates and the results are given in Table I. Neither complex possesses TAP geometry, although it is rather closely approached by diamagnetic [Fe(phen)$_3$]$^{2+}$. The order of increasing ϕ, Fe(II) > Ni(II), is the same as in series 4 and the twist angles correspond closely to those of the (py)$_3$tren complexes of these ions. Provided that interligand interactions, especially those among hydrogens proximal to nitrogen, are of similar magnitude, this comparison implies that [M((py)$_3$tren)]$^{2+}$ are not constrained to any significant degree toward a TP structure.

Potentially stable geometries of sterically unencumbered chelate complexes, as influenced by d-electron energetics, have been investigated by use of the AOM.[33,36] This model allows calculation of d-orbital energies perturbed by covalent bonding as a function of bite and twist angles. The general ligand-field matrix element is

$$\langle d_i | V_{\text{LF}} | d_j \rangle = \sum_{\lambda\omega} \sum_{n=1}^{N} e_{\lambda n} F_{\lambda\omega}(d_i, L_n) F_{\lambda\omega}(d_j, L_n) \qquad (5)$$

---

(34) As illustrated in Figure 2, ψ is also that angle by which the coordinate system (x_1, y_1, z_1) must be rotated around z_1 in order to place the y_1 axis parallel to the π^s ligand orbitals after moving the ligand atom from P_1 by a rotation θ around the y axis and a rotation $\phi/2$ around the z axis. In TP geometry $\psi = \phi = 0°$. In a nonprismatic disposition of ligands with L_1 and L_4 at P_1'' and P_4'', ψ is also the angle between y_1'' and the π^s orbitals if the rotation of (x_1, y_1, z_1) around z_1 were not performed. The angle ψ corresponds to the angle β used by Tomlinson[35] in his discussion of tris chelates.

(35) A. A. G. Tomlinson, *J. Chem. Soc. A*, 1409 (1971).

(36) C. E. Schäffer and C. K. Jørgensen, *Mol. Phys.*, **9**, 401 (1965); C. E. Schäffer, *Proc. Roy. Soc., Ser. A*, **297**, 96 (1967).

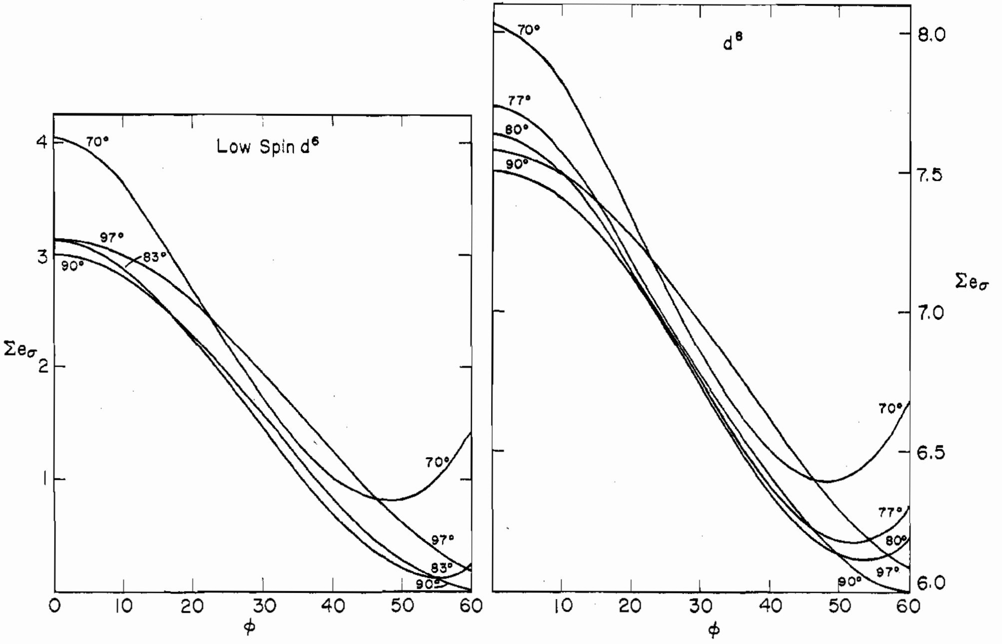

Figure 4.—Sums of one-electron d-orbital energies for d^8 and low-spin d^6 $M(L{-}L)_3$ complexes with various bite angles as a function of the twist angle ϕ.

where the first summation includes metal–ligand bonding involving ligand σ, π^s, and π^c (in-plane) orbitals. N is the total number of ligand atoms. $F_{\lambda\omega}$ is the factor by which the angular overlap integral is diminished from maximum value, and $e_{\lambda n}$ (e_σ, e_{π^s}, e_{π^c}) are empirical energy units. Calculations were performed using a computer program of local origin. Values of $F_{\lambda\omega}$ (d_i, $L_n(\theta, \phi, \psi)$) were taken from the tabulation of Schäffer[33] and angular coordinates were calculated from eq 1 and 2. One-electron d-orbital energies as a function of twist for constant bite angles of 77 and 90° are given in Figure 3. The former angle is typical of those found for complexes **1–4** with various values of ϕ. For $\alpha < 90°$ the energy orders in the TP and TAP limits are $a_1' < e' < e''$ and $e_a \lesssim a_1 < e_b$, respectively, and are unchanged by inclusion of moderate amounts of stabilizing ($e_{\pi^s} = -0.1e_\sigma$) or destabilizing ($e_{\pi^s} = 0.1e_\sigma$) π bonding. Orbital ordering in the prismatic limit is the same as that obtained from ionic model calculations.[10,35] Variation of energies as a function of ϕ is not strictly comparable with previous results,[10] which did not include the effects of simultaneous changes of θ and ϕ with a constant α. Shown in Figure 4 are sums of one-electron σ-bonding energies for the d^8 and low-spin d^6 configurations as ϕ is varied from 0 to 60°. Bite angles are varied from 70 to 97° to cover the complexes[7] previously mentioned, those in Table I, and species such as $Co(acac)_3$ ($\alpha = 97°$[37]). For $\alpha < 90°$ shallow minima are obtained in the *ca.* 48–56° range of ϕ values.[38] It is within or somewhat to the low side of this interval that stable geometries of $[M(phen)_3]^{2+}$, $[M((py)_3tren)]^{2+}$ (M = Fe(II), Ni(II)) and other low-spin d^6 species[7] are found in the solid state. All of these complexes possess the common feature of bite angles substantially less than 90°, which are determined by the bite distances of the relatively rigid unsaturated ligands and the metal–ligand distances. For the two configurations shown in Figure 4, the calculations indicate that, provided $\alpha < 90°$, maximum angular overlap (minimum d-electron destabilization) will in general occur at twist angles less than 60°.

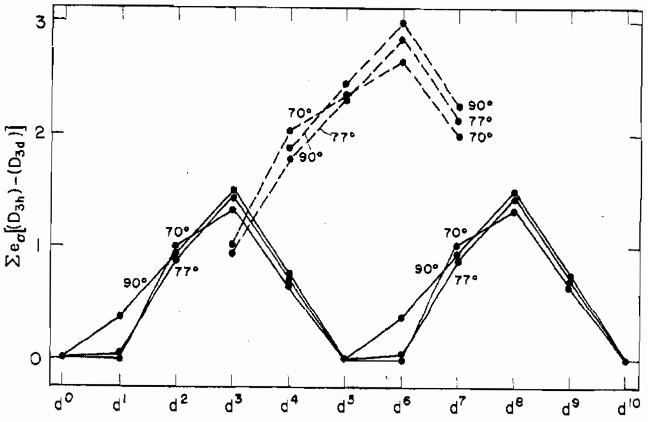

Figure 5.—Differences in destabilization energies for the complex $M(L{-}L)_3$ (α = 70, 77, 90°) in TP (D_{3h}) and TAP (D_{3d}) geometries as a function of the number of d electrons. The effects of π bonding are not included: high spin, ——; low spin, - - - -.

To provide a partial basis for the interpretation of series 4, differences in total d-electron energies due to σ bonding in the TP and TAP geometries have been calculated for the d^{0-10} configurations using the AOM. The results are shown in Figure 5 and are not substantially altered by inclusion of moderate amounts of π bonding (*vide supra*) or selection of $\phi \approx 50°$ as one structural limit. Stabilization energy differences are meaningful only if spin states are the same in the limiting geometries and any Jahn–Teller distortions are small perturbations on the trigonal symmetry. The plot of Δ(LFSE) *vs.* d^n calculated by Gillum, *et al.*,[10] using a simplified ionic model approximates those

---

[37] E. C. Lingafelter and R. L. Braun, *J. Amer. Chem. Soc.*, **88**, 2951 (1966).

[38] Inclusion of stabilizing metal–π^s bonding shifts these minima to smaller values of ϕ.

TABLE III

MAGNETIC AND SPECTRAL DATA FOR TRIGONAL NICKEL(II) AND COBALT(II) COMPLEXES

Compound	μ_{eff},^{a} BM	λ_{max}, cm^{-1} (ϵ)^{b,e}
$[Ni(PccBF)](BF_4)$	3.11	9380 (28), 11,000 (27), ∼20,500 sh (50), ∼22,200 sh (80), ∼29,000 sh (3300), 34,500 (14,700), 38,000 (24,000)
$[Ni((py)_3tach)](ClO_4)_2$	3.13	11,000 (27), 12,000 (25), 19,000 (48), ∼31,500 sh (5400), 36,000 (17,100)
$[Ni((py)_3tame)](ClO_4)_2$	3.06	∼11,400 sh (22), 12,400 (30), ∼19,500 sh (60), ∼27,500 sh (450), 36,000 (19,900)
$[Ni((py)_3tren)](ClO_4)_2$	3.12	11,630 (7.9), 12,550 (7.7), 18,300 (12), 27,500 (1380), 36,000 (18,100)
$[Ni(P(CH_3pox)_3)](ClO_4)_2$	2.99	10,500^d (17), ∼11,700^d sh (14), 18,600^d (15), 34,500 (19,900)
$[Ni(P(bipy)_3)](ClO_4)_2$	3.12	10,800 (20), ∼11,900 sh (17), 18,500 (18), ∼25,000 sh (∼200), ∼32,000 sh (19,000), 33,500 (28,000)
$[Ni(P(py)_3)_2](ClO_4)_2$	3.06	∼11,500 sh (4.0), 12,600 (4.9), 19,000 (6.4), ∼26,000 sh (∼200), 29,000 (1080), 37,000 (25,800), ∼38,000 sh (20,000)
$[Co(PccBF)](BF_4)$	4.91	8130 (3.6), 11,800^c (6.3), 14,250^c (5.7), ∼22,000 sh (230), 27,000 (2500), 35,300 (16,000), ∼38,000 (24,000)
$[Co((py)_3tach)](ClO_4)_2$	4.90	9380 (8.1), ∼15,500^c sh (5.8), ∼20,400 sh (70), ∼21,600 sh (120), ∼29,000 sh (2300), 36,000 (15,800)
$[Co((py)_3tame)](ClO_4)_2$	4.95	∼11,000 sh (22), 19,500 (500), 29,000 (2570), 36,000 (16,600)
$[Co((py)_3tren)](ClO_4)_2$	4.52	10,900 (11), ∼15,500^c (2.8), ∼19,500 sh (180), 28,000 (2880), 36,000 (22,600)
$[Co(P(CH_3pox)_3)](BF_4)_2$	4.70	9400 (8.4), ∼13,500^c sh (3.4), ∼21,000 sh (47), ∼29,000 sh (4000), 34,500 (16,900)
$[Co(P(bipy)_3)](ClO_4)_2$	4.77	9600 (7.1), 15,600^c (4.8), ∼20,300 sh (28), 21,500 (33), ∼29,000 sh (5000), 33,800 (25,000)
$[Co(P(py)_3)_2](ClO_4)_2$	4.76	11,000 (3.9), 21,800 (25), ∼31,000 sh (3000), 37,000 (28,000)

[a] Solid state, ∼25°. [b] Acetonitrile solution. [c] Demonstrated or suspected Co(I) bands. [d] Acetone solution. [e] Intensities uncorrected for underlying absorption.

in the figure. While a full array of complexes necessary to test conclusions drawn from relative stabilization energy differences is not available, we concur with an earlier statement,[10] made on the basis of less structural data, that these differences provide a partial explanation of existing stereochemical trends. Thus, the Fe(II) complexes **1**, **3**, and **4** are all substantially displaced toward the antiprism to an extent greater than for any other metal ion coordinated to the same ligand. Based on isomorphism relationships, it would appear that in the $(py)_3$tame series[19a] Ni(II) and Co(II) might have comparable structures and that in the $(py)_3$tach series[10,19b] Ni(II) less closely approaches the prismatic limit than does Co(II). Other than in the trivial $d^{0,10}$ and high-spin d^5 cases, d-electron energies in the two limiting geometries are nearly the same only for d^1 and high-spin d^6 ions, especially in complexes with $\alpha < 90°$. No such complexes of types **1–4** have as yet been prepared.

Relative energies of the various d^n configurations are of course not the only factor affecting the stereochemical trend expressed by series 4. It is noted that this series also reflects variation in effective ionic radius, with Zn(II) being *ca.* 0.15 Å larger than low-spin Fe(II). Equation 1 may be rewritten to express the relationship of the twist angle and the structural parameters of the coordination sphere d, r (metal–ligand distance), and s (length of a triangular edge); $s = \sqrt{3}r \sin \theta$.

$$\cos \phi/2 = [3r^2 - {}^3/_4 d^2]^{1/2}/s \qquad (6)$$

Equivalent forms of eq 1 and 6 have been obtained independently.[7j] The effect on ϕ of varying ionic radii cannot be quantitatively analyzed due to the number of parameters involved. However, the qualitative implications of changes in r can be seen if a rigid ligand system is assumed such that d and s are constant with ϕ. Twist angles in two complexes containing the ions M′ and M are then related by, *e.g.*, eq 7.

$$\cos^2 (\phi/2)_{M'} = 3(r_{M'}{}^2 - r_M{}^2)/s^2 + \cos^2 (\phi/2)_M \qquad (7)$$

If the M complex, characterized by particular ϕ, s, and d values, is considered essentially strainless, the effect of altering the metal–ligand distance upon passing to the M′ complex is readily estimated. Using observed r values and other structural data[9c] for $[Zn(PccBF)]^+$, ϕ is estimated as 53° for $[Fe(PccBF)]^+$ if the cage were fully capable of responding to changes in r only. A slightly better comparison involves $[Co(dmg)_3(BF)_2]^{1+,0}$, in which s and d are more nearly constant.[12] The Co(II) complex (ϕ = 8.6°) is thought to be only slightly strained.[12] For the Co(III) complex ϕ is estimated as 39°, compared to the observed 22°. This argument, while quite approximate and expressible in other equivalent ways, suggests that in a series of complexes of the same ligand decrease in ionic radii will increase twist angles as the metal ions seek to achieve optimum metal–ligand distances.[39] Thus the order of metal ions in series 4 would appear to result from a combination of d-electron stabilization and metal ion size effects, which, at least for Fe(II) and Zn(II), parallel each other.

Establishment of series 3 in the solid state for certain M(II) ions has led to an examination of the electronic and pmr spectra and polarography of complexes **1–4** and **7** in solution. Co(II) and Ni(II) complexes have been studied in the most detail. Changes in certain spectral features and redox potentials with structure, described below, have been observed. Similar data for complexes **5** ($[M(P(CH_3pox)_3)]^{2+}$) and **6** ($[M(P(bipy)_3)]^{2+}$), whose solid-state structures are unknown, have been obtained and approximate struc-

---

(39) In a series of alkali metal cryptate complexes the twist angles increase in the order $Cs^+ = Rb^+ < K^+ < Na^+$: B. Metz, D. Moras, and R. Weiss, *Chem. Commun.*, 444 (1971). The structures are intermediate between a bicapped TP and bicapped TAP. However, the M–O distances are not necessarily optimal due to the size of the O_6N_2 cage.

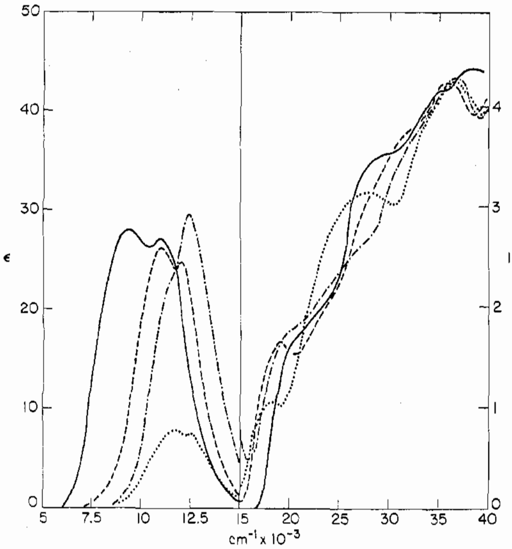

Figure 6.—Electronic absorption spectra of the sexadentate Ni(II) complexes 1–4 in acetonitrile: ——, [Ni(PccBF)](BF$_4$); - - - -, [Ni((py)$_3$tach)](ClO$_4$)$_2$; —·—·, [Ni((py)$_3$tame)](ClO$_4$)$_2$; ····, [Ni((py)$_3$tren)](ClO$_4$)$_2$.

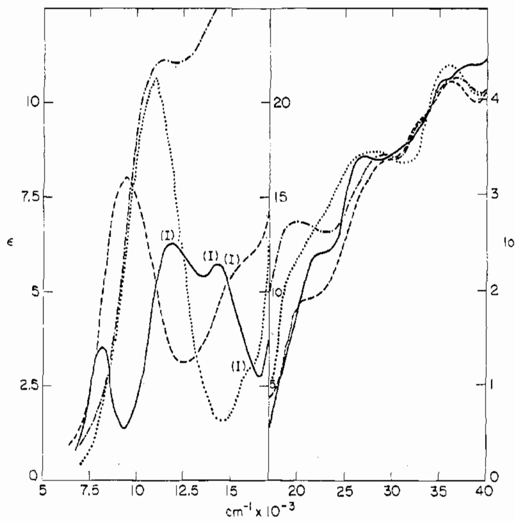

Figure 7.—Electronic absorption spectra of the sexadentate Co(II) complexes 1–4 in acetonitrile: ——, [Co(PccBF)](BF$_4$); - - - -, [Co((py)$_3$tach)](ClO$_4$)$_2$; —·—·, [Co((py)$_3$tame)](ClO$_4$)$_2$ (right hand intensity scale, 5000–15,000 cm^{-1}); ····, [Co((py)$_3$tren)](ClO$_4$)$_2$. The designation (I) refers to demonstrated or suspected Co(I) bands.

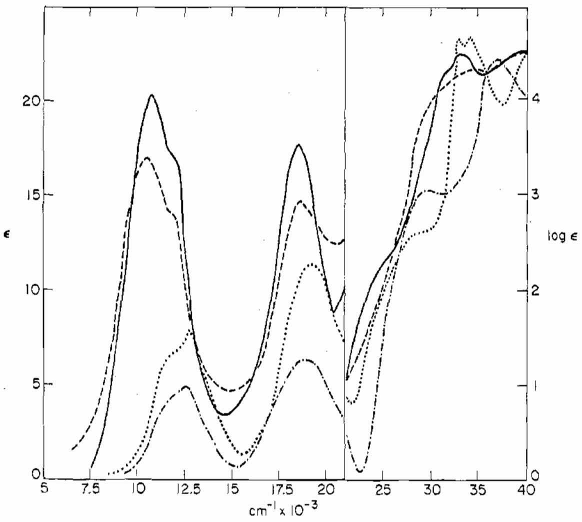

Figure 8.—Electronic absorption spectra of Ni(II) complexes 5–7 in acetonitrile: ——, [Ni(P(bipy)$_3$)](ClO$_4$)$_2$; - - - -, [Ni(P-(Mepox)$_3$)](ClO$_4$)$_2$ (5000–20,000 cm^{-1} in acetone); —·—·, [Ni(P(py)$_3$)$_2$)](ClO$_4$)$_2$; ····, [Ni(bipy)$_3$](ClO$_4$)$_2$.

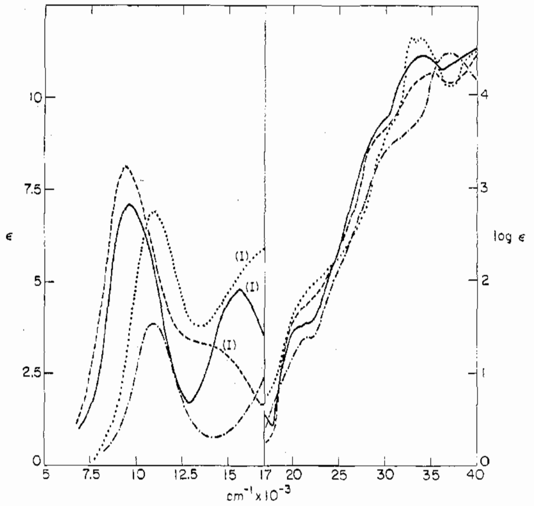

Figure 9.—Electronic absorption spectra of Co(II) complexes 5–7 in acetonitrile: ——, [Co(P(bipy)$_3$)](ClO$_4$)$_2$; ——, [Co-(P(Mepox)$_3$)](ClO$_4$)$_2$; —·—·; [Co(P(py)$_3$)$_2$](ClO$_4$)$_2$; ····, [Co-(bipy)$_3$](ClO$_4$)$_2$. The designation (I) refers to suspected Co(I) bands.

tures in solution are proposed. The complexes **7**, [M(P(py)$_3$)$_2$]$^{2+}$, have been included because, unlike the species **1**, **5**, and **6** having related tripyridylphosphine ligand fragments, they are not sterically constrained from achieving full TAP geometry.

Electronic Spectra.—Spectra of certain complexes of types **2**,[10,14] **3**,[19a] and **4**[11a] and for [M(bipy)$_3$]$^{2+}$,[40] not measured under the same experimental conditions in all cases, have been reported. In order to obtain a careful comparison of band positions and intensities, spectra of the Co(II) and Ni(II) complexes **1**–**4** and **7** and the tris(bipyridyl) complexes were measured in acetonitrile solution. Data are given in Table III and spectra are shown in Figures 6–9. There was no significant disparity between the solution and solid-state (mull) spectra of complexes **1**–**7** except for an *ca.* 1000 cm^{-1} red shift of the bands of crystalline [Co-((py)$_3$tach)](ClO$_4$)$_2$ compared to the solution spectrum. It was therefore concluded that no gross differences exist between solid state and solution structures, with the possible exception of the [Co((py)$_3$-tach)]$^{2+}$.

(a) **Nickel(II) Complexes.**—Spectra of complexes which most closely approach the TP and TAP limits are first considered. A variety of tris(α-diimine) complexes have been previously examined by Robinson, Curry, and Busch,[41] who interpreted the spectra in O_h symmetry and obtained Dq values ranging from 1040 to 1280 cm^{-1}. They have also provided reasonable evidence that the less intense feature at 11,400–12,200 cm^{-1} is the spin-forbidden $^3A_{2g} \rightarrow {}^1E_g(D)$ transition, whose energy is predicted to be essentially

---

[40] R. A. Palmer and T. S. Piper, *Inorg. Chem.*, **5**, 864 (1966).

[41] M. A. Robinson, J. D. Curry, and D. H. Busch, *ibid.*, **2**, 1178 (1963).

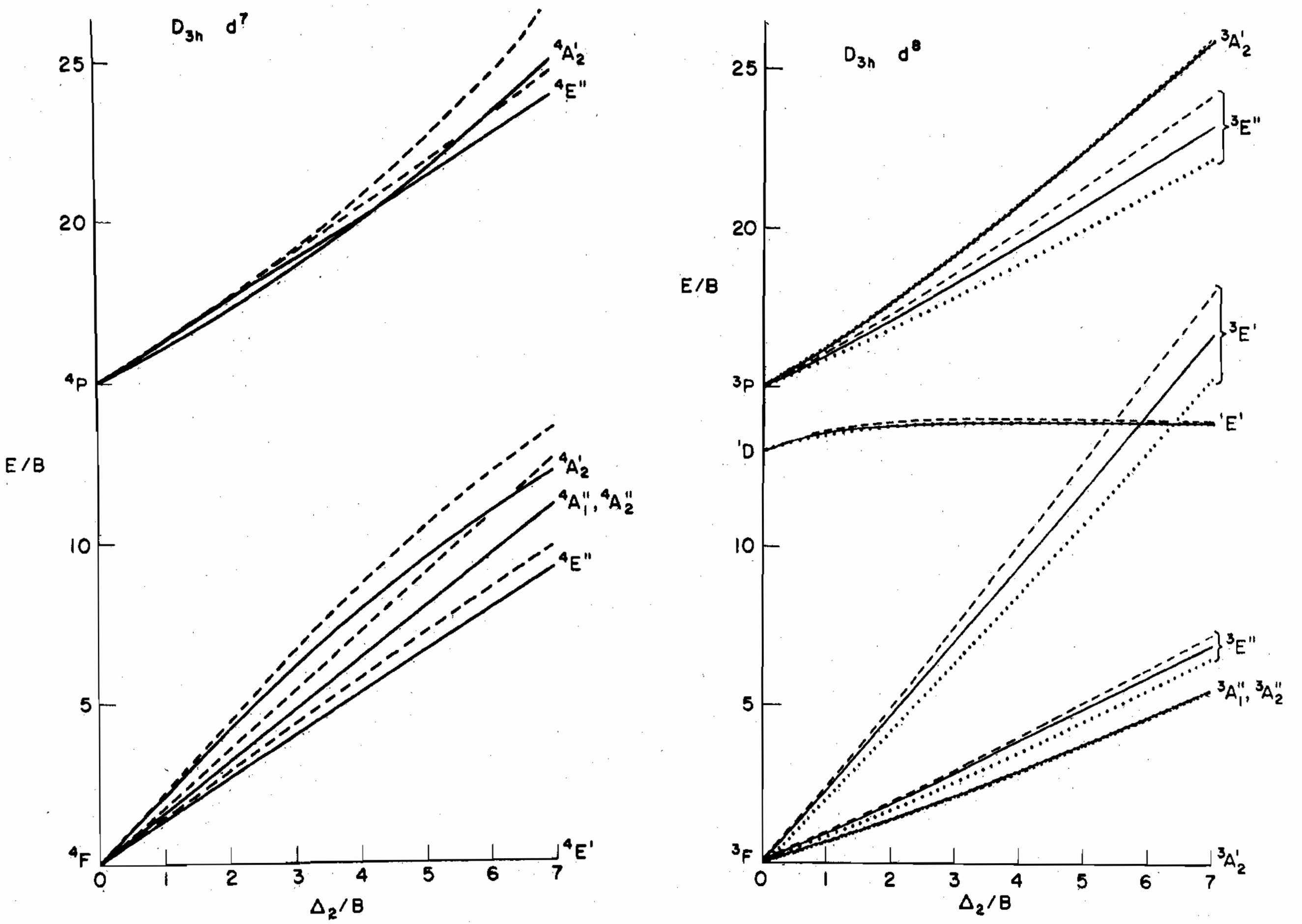

Figure 10.—Energy-level diagrams for d^7 (high-spin) and d^8 configurations in D_{3h} symmetry for $C/B = 4.0$ and selected Δ_1/Δ_2 ratios: · · · ·, 0.4; ——, 0.6; - - - -, 0.8. The designation of states is not the same as that employed elsewhere[10] and follows common group theoretical usage.[45a]

independent of ligand-field strength by the Tanabe–Sugano treatment[42] when $Dq/B \gtrsim 1.5$. The spectrum of $[Ni((py)_3tren)]^{2+}$, shown in Figure 6, can be analyzed assuming octahedral microsymmetry and the following energies and assignments accord well with earlier results[21b] for other salts in different solvents: ${}^3A_{2g} \rightarrow {}^3T_{2g}$ (ν_1), 12,550 cm^{-1}; $\rightarrow {}^3T_{1g}(F)$ (ν_2); 18,300 cm^{-1}; $\rightarrow {}^1E_g({}^1D)$, 11,630 cm^{-1}; Dq = 1255 cm^{-1}, B = 710 cm^{-1}. Intense absorptions at higher energies obscure the octahedral ν_3 band (${}^3A_{2g} \rightarrow {}^3T_{1g}(P)$). The spectrum of $[Ni(P(py)_3)_2]^{2+}$ [43] (Figure 8) can be assigned similarly, with Dq = 1260 cm^{-1} and B = 690 cm^{-1}. The spin-forbidden band is assigned to the 11,500 cm^{-1} feature. These data, together with those for $[Ni(bipy)_3]^{2+}$ [21b,40] (Dq = 1270 cm^{-1}, B = 710 cm^{-1}) and related complexes,[41] serve to characterize the α-diimine $Ni-N_6$ chromophore of TAP or near-TAP geometry. In none of the solution spectra were additional splittings of ligand-field bands due to a trigonal component evident.[44]

Crystal-field calculations for five-[45] and six-coordinate[10,35,46] complexes of D_{3h} symmetry have been undertaken. The treatment of Gillum, *et al.*,[10] which is the most pertinent here, was carried out for the special case of TP coordination with θ = 54.79°. Selection of this polar angle causes the term in the ligand-field potential containing the second-order spherical harmonics to vanish and the one-electron orbital energy differences Δ_1 and Δ_2 to be equal. Within the one-electron approximation a less restricted treatment

$$\Delta_1 = E(e') - E(a_1') \qquad \Delta_2 = E(e'') - E(e') \qquad (8)$$

of the spectra of complexes with D_{3h} microsymmetry can be achieved with AOM calculations, which allow exact geometries to be readily taken into account. Procedures for such calculations are outlined in the Appendix where, in addition, it is concluded that a reasonable range for the ratio Δ_1/Δ_2 is 0.4–0.8. To provide a guide for spectral interpretations of the d^8 case, energy-level diagrams calculated using ratios in this range are given in Figure 10. Of the singlet states from ${}^1D$ only ${}^1E'$ is included; the others (${}^1A_1'$, ${}^1E''$) occur at higher energies. Electric dipole selection rules for D_{3h} symmetry are the following. Only transitions to the A_1'' and E' states are allowed. If

$$A_2' \not\rightarrow A_2'', E'', A_2' \quad A_2' \xrightarrow{\parallel} A_1'' \quad A_2' \xrightarrow{\perp} E'$$

---

(42) Y. Tanabe and S. Sugano, *J. Phys. Soc. Jap.*, **9**, 753, 766 (1954).

(43) The data for this complex are in close agreement with the spectral results for $[Ni(N(py)_3)_2](ClO_4)_2$: (a) G. C. Kulasingam, J. C. Lancaster, W. R. McWhinnie, and J. B. Watts, *Spectrochim. Acta, Part A*, **26**, 835 (1970); (b) W. R. McWhinnie, G. S. Kulasingam, and J. C. Draper, *J. Chem. Soc. A*, 1199 (1966).

(44) If the structure of $[Ni(bipy)_3]^{2+}$ is comparable to that of $[Ni(phen)_3]^{2+}$ (Table I), the near degeneracy of the a_1 and e_a orbitals at $\phi \approx 50°$ offers a plausible explanation of the lack of resolvable splitting of the octahedral ν_1 band ($t_{2g}^6e_g^2 \rightarrow t_{2g}^5e_g^3$ parentage) in the single-crystal spectrum of the former.[40] Polarizations were observed to follow selection rules appropriate to D_3 symmetry.

(45) (a) M. Ciampolini, *Inorg. Chem.*, **5**, 35 (1966); (b) J. S. Wood, *ibid.*, **7**, 852 (1968).

(46) P. H. Davis and J. S. Wood, *Chem. Phys. Lett.*, **4**, 466 (1969).

the microsymmetry is reduced to C_{3v}, which more closely approximates that actually found in [Ni(PccBF)]$^+$, the selection rules are $A_2 \rightarrow A_2$ (||), E(⊥), A_1 (forbidden).

The solution spectrum of [Ni(PccBF)]$^+$ is shown in Figure 6. The near-TP chromophore gives rise to three features whose intensities suggest identification as ligand-field bands. Those at 9380 and 11,000 cm^{-1} are both polarized perpendicular to the molecular pseudo-C_3 axis in the single-crystal spectrum, consistent with the assignments $^3A_2' \rightarrow {}^3E'$, $^1E'$ in D_{3h} microsymmetry. Resolution of these bands by curve-fitting indicates that the higher energy feature is the spin-forbidden transition, which presumably has borrowed intensity from the spin-allowed transition. The unpolarized shoulder at ~20,500 cm^{-1} is tentatively assigned to the $^3A_2' \rightarrow {}^3E''$ and/or $^3A_2'$ transition(s), both of which are forbidden. Palmer and Piper[40] report a possibly analogous partial breakdown of D_3 selection rules for the 19,000-cm^{-1} band of [Ni(bipy)$_3$]$^{2+}$. Assignment of the $^3E'$, $^1E'$ transitions is consistent with the d^8 energy-level scheme in Figure 10 with $\Delta_1/\Delta_2 = 0.6$–0.8. For $\Delta_1/\Delta_2 = 0.6$, $B \approx 800$ cm^{-1} and $\Delta_2 \approx 4000$ cm^{-1}. Transitions to $^3A_1''$, $^3A_2''$, and $^3E''$ are predicted to occur below about 4000 cm^{-1}. No other electronic bands could be located in the crystal or solution spectra down to 5000 cm^{-1}. The energies of the upper $^3E''$ and $^3A_2'$ states are predicted to be in the range of *ca.* 16,500–18,000 cm^{-1}, which is in only fair agreement with the feature observed at ~20,500 cm^{-1}. An alternative assignment of the 9380 and 11,000 cm^{-1} bands to the first three triplet states disagrees with the polarization data and requires values of B in excess of the free ion value by a factor of *ca.* two. This assignment is rejected.

Interpretation of the spectral differences among the Ni(II) complexes **1**–**4**, **7**, and [Ni(bipy)$_3$]$^{2+}$ has been attempted by the use of energy level schemes calculated for the ϕ range of 0° to 60° (see Appendix). An illustrative diagram of this type, calculated for a constant bite angle of 77° and no π bonding, is shown in Figure 11. Each complex exhibits a band in the narrow 11,000–11,700 cm^{-1} region which is assigned to the $^3A_2 \rightarrow {}^1E$ transition inasmuch as the calculations indicate that the energy of the singlet state is essentially independent of ϕ. The spectral features most clearly affected by structural changes are the energies and intensities of the spin-allowed bands in the 9000–13,000 cm^{-1} region. The energies show a blue shift, with those of [Ni((py)$_3$tach)]$^{2+}$ (12,000 cm^{-1}) and [Ni((py)$_3$tame)]$^{2+}$ (12,400 cm^{-1}) intermediate between the values for TAP and TP species. Intensities are two to three times smaller in TAP complexes of effective octahedral (centrosymmetric) microsymmetry than in complexes of TP or intermediate stereochemistry.[47] A satisfactory interpretation of these bands in the two complexes of intermediate stereochemistry and, hence, of the shift of bands in this region to higher energy with increasing twist angle, has not been achieved using the range of parameters indicated in the Appendix. In particular, it has not been possible to accommodate the relative energies of the $^3A'_2 \rightarrow {}^3E'$ and $^3A_2 \rightarrow {}^3E$, $^3A_1$ (octahedral ν_1) bands observed in the TP and TAP chromophores, respectively. This situation, together with the sensitivity of the ^1E energy to the parameterization of e_σ in terms of B, does not allow definite assignment of the spin-allowed transitions to either of the lower ^3E states or to the $^3A_2$ state. The calculations are clearly simplified in that α and B are considered independent of ϕ, and no account has been taken of departure from effective $D_{3(d)}$ symmetry, which is particularly marked in the case of [Ni((py)$_3$tach)]$^{2+}$. Pending more detailed calculations and determination of polarized crystal spectra, the matter of specific assignments of the ligand-field bands of [Ni((py)$_3$tach)]$^{2+}$ and [Ni((py)$_3$tame)]$^{2+}$, including those in the 19,000–20,000-cm^{-1} range, remains open. However, within the present series of α-diimine complexes the energy order of the spin-allowed bands at 9000–13,000 cm^{-1} serves as an empirical indicator of structural change from the TP to the TAP configuration.

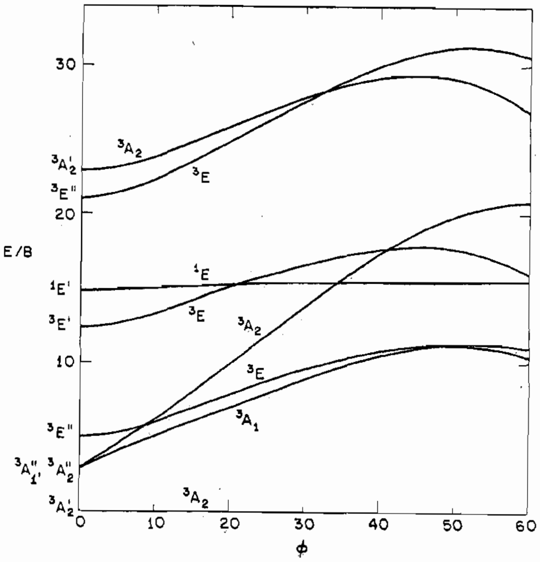

Figure 11.—Energy-level diagram for the d^8 configuration in the interval $0° \leqslant \phi \leqslant 60°$. Calculations were performed with $\alpha = 77°$, $e_\sigma = 4B$, $e_{\pi^s} = e_{\pi^c} = 0$, and $C = 4B$.

(b) **Cobalt(II) Complexes.**—Spectra of the complexes **1**–**4** are shown in Figure 7 and those of [Co(bipy)$_3$]$^{2+}$ and [Co(P(py)$_3$)$_2$]$^{2+}$ are given in Figure 9. Energy-level diagrams for D_{3h} symmetry including quartet states only are depicted in Figure 10. Analysis of the spectra of these complexes is hampered by the availability of detailed structural data for only [Co((py)$_3$tren)]$^{2+}$ and [Co(PccBF)]$^+$, and the occurrence of spurious bands known or suspected to arise from highly absorbing Co(I) impurities. The spectra of [Co(bipy)$_3$]$^{2+}$ and [Co(P(py)$_3$)$_2$]$^{2+}$ are taken as those of TAP chromophores and may be assigned in octahedral microsymmetry. For the former $Dq = 1270$ cm^{-1} and $B = 790$ cm^{-1}.[40] Analogous treatment of [Co(P(py)$_3$)$_2$]$^{2+}$ leads to the following assignments and parameters: $^4T_{1g} \rightarrow {}^4T_{2g}$ (ν_1), 11,000 cm^{-1}; $\rightarrow {}^4T_{1g}(P)$ (ν_3), 21,800 cm^{-1}; $Dq = 1260$ cm^{-1}, $B = 810$ cm^{-1}. The structure of [Co(PccBF)]$^+$ approximates TP geometry but, unlike other complexes of this type, all three twist angles are different. Its spectrum in the near-infrared and visible regions consists of four bands.

---

[47] This statement refers only to the series of complexes under consideration. Other Ni–N$_6$ TAP complexes with diimine-type ligands can have larger extinction coefficients. As one example, bis(2,6-diacetylpyridyldioximo)nickel(II) has ϵ ~30 for its octahedral ν_1 band: E. I. Baucom and R. S. Drago, *J. Amer. Chem. Soc.*, **93**, 6469 (1971).

TABLE IV

PROTON ISOTROPIC SHIFTS[a] AND LINE WIDTHS FOR TRIGONAL NICKEL(II) COMPLEXES IN ACETONITRILE-d_3 AT ∼29°

Compound	Shift, ppm (line width, Hz) 3-H	4-H	5-H
$[Ni(PccBF)](BF_4)$	−57.0 (24)	−14.75[b] (35)	−24.3 (180)
$[Ni((py)_3tach)](ClO_4)_2$	−42.15[c] (65)	−7.40[d] (43)	−38.63[e] (180)
$[Ni((py)_3tame)](ClO_4)_2$	−43.35[f] (230)	−7.96[g] (52)	−40.35 (250)
$[Ni((py)_3tren)](ClO_4)_2$	−40.80[h] (300)	−7.25[i] (73)	−44.70 (300)
$[Ni(bipy)_3](ClO_4)_2$	−52.60 (450)	−6.32 (72)	−37.73 (320)
$[Ni(P(py)_3)_2](ClO_4)_2$[j]	−38.0 (500)	−8.5 (90)	−30.7 (400)
$[Ni(P(bipy)_3)](ClO_4)_2$	−54.6 −66.5 (∼80)	−6.90 −7.77 (∼40)	−32.9 (∼180)

[a] Diamagnetic shifts (3-H, 4-H, 5-H) for the first four complexes taken from spectra of analogous Zn(II) or Fe(II) complexes: **1**, Zn(II) (−7.9, −8.3, −8.3); **2**, Fe(II) (−6.7, −7.5, −8.1); **3**, Fe(II) (−7.3, −7.5, −8.1); **4**, Fe(II) (−7.0, −7.5, −8.2 ppm). Ring proton shifts of the last three compounds and all methyl shifts are referenced to the free ligands. [b] 4-CH_3 at +16.4 ppm. [c] 3-CH_3 at −1.1 ppm. [d] 4-CH_3 at +9.85 ppm. [e] 5-CH_3 at −1.5 ppm. [f] 3-CH_3 at −1.1 ppm. [g] 4-CH_3 at +10.8 ppm. [h] 3-CH_3 at −1.3 ppm. [i] 4-CH_3 at +10.2 ppm. [j] In DMSO-d_6.

Those at 11,800 and 14,250 cm^{-1} were shown to arise from Co(PccBF), which is readily generated from the monocation by electrochemical reduction[48] (*vide infra*). The remaining bands at 8130 and ∼22,000 cm^{-1} may arise from transitions to the two separated sets of quartet states (Figure 10), although the narrowness of the low-energy band is not indicative of multiple transitions. The related features in the spectrum of $[Co((py)_3tach)]^{2+}$, which in solution occur at 9380 and ∼20,400 cm^{-1}, have been similarly assigned assuming TP geometry.[10] The spectrum of $[Co((py)_3tren)]^{2+}$ is the most similar to those of the foregoing TAP complexes and, assuming $\nu_1 = 10{,}900\ cm^{-1}$ and $\nu_3 = 19{,}500\ cm^{-1}$, it can be approximately fit to O_h microsymmetry with $Dq \approx 1200\ cm^{-1}$ and $B \approx 650\ cm^{-1}$. The actual structure of this complex deviates considerably from this idealized symmetry, however, having $\phi = 49°$ and an apical Co–N distance of 2.87 Å.[22b] As with the corresponding Ni(II) complexes, the first spin-allowed band, which occurs in the 8000–11,000 cm^{-1} interval, displays a shift to higher energies upon passing from the TP to the TAP structures. In view of the coincidence of this band (∼11,000 cm^{-1}) in $[Co((py)_3tren)]^{2+}$ and $[Co((py)_3tame)]^{2+}$ and the lack of a precise structure for $[Co((py)_3tach)]^{2+}$, it cannot be ascertained at present if this shift is monotonic with increasing twist angle.

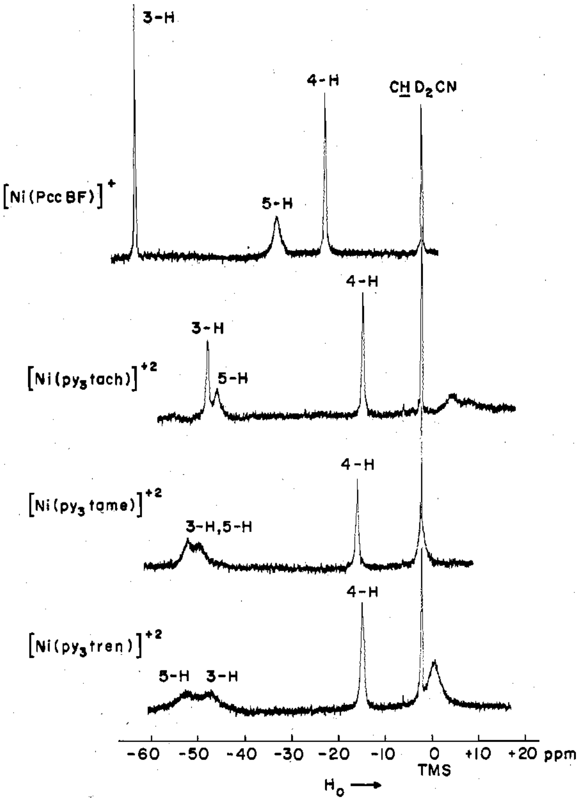

Figure 12.—Pmr spectra (100 MHz) of Ni(II) complexes **1**–**4** in CD_3CN at ∼29°. Signals of $[Ni((py)_3tach)]^{2+}$ and $[Ni((py)_3tren)]^{2+}$ near or upfield of TMS are due to aliphatic protons. A similar resonance of $[Ni((py)_3tame)]^{2+}$ is partially obscured by the solvent signal.

Pmr Spectra.—Inasmuch as isotropically shifted ligand proton resonances can serve as sensitive probes of structures and small structural differences in paramagnetic complexes,[49] the pmr spectra of Ni(II) and Co(II) complexes ranging over the accessible structural extremes have been examined. Isotropic shifts and line widths for the Ni(II) complexes are set out in Table IV; spectra of the Ni(II) series **1**–**4** in acetonitrile are shown in Figure 12. The spectrum of $[Ni(bipy)_3]^{2+}$ in D_2O has been previously assigned.[50] For the complexes **1**–**4** and $[Ni(P(py)_3)_2]^{2+}$ three peaks are located in the range −10 to −70 ppm from TMS. By analogy to $[Ni(bipy)_3]^{2+}$, these arise from ring protons 3-H, 4-H, and 5-H. Using the methyl derivatives listed in Table II and in the Experimental Section, specific assignments were made for complexes **2**, **3**, and **4**. The 4-H signal of $[Ni(PccBF)]^+$ was identified by similar means. 3-H and 5-H signals were assigned by line width comparisons with corresponding resonances of $[Ni((py)_3tach)]^{2+}$, whose ring proton signals were

---

(48) Electrolysis at −0.5 V *vs.* sce (*cf.* Table V) caused a marked increase in the intensities of these features. Spectral measurement of a solution subjected to prolonged reductive electrolysis indicated that the sample whose spectrum is shown in Figure 7 contained *ca.* 0.6% of the Co(I) complex. Electrochemical oxidation failed to remove completely this material. Its presence in all samples of the Co(II) salt which we have prepared led to inconclusive results in single-crystal polarized spectral measurements. Additional experiments using acetonitrile solutions indicated that the Co(I) complex could also be generated photolytically, as appears to be the case for $[Co(bipy)_3]^{2+}$.[40] The shoulder at ∼16,000 cm^{-1} in the spectrum of $[Co(bipy)_3]^{2+}$ in Figure 9 and in that reported earlier[40] coincides with the 16,400-cm^{-1} band of $[Co(bipy)_3]^+$ (Y. Kaizu, Y. Torii, and H. Kobayashi, *Bull. Chem. Soc. Jap.*, **43**, 3296 (1970)). An additional band of the latter at 7200 cm^{-1} was not detected, however. Bands suspected to be due to Co(I) impurities in other complexes are so designated in Figures 7 and 9 and in Table III.

(49) D. R. Eaton and W. D. Phillips, *Advan. Magn. Resonance*, **1**, 103 (1965); R. H. Holm, *Accounts Chem. Res.*, **2**, 307 (1969); G. N. La Mar and L. Sacconi, *J. Amer. Chem. Soc.*, **89**, 2282 (1967).

(50) M. Wicholas and R. S. Drago, *ibid.*, **90**, 6946 (1968). Differences in solvent between this work and ours produce small changes in line widths and shifts. The 6,6′-H signal could not be located with the concentrations employed in the present study.

unambiguously assigned by methyl substitution at the 3-, 4-, and 5-positions. Assignments for $[Ni(P(py)_3)_2]^{2+}$ were obtained by analogy of line widths and shifts with the bipyridyl complex. Due to solubility limitations the spectrum of the former was obtained in DMSO, in which line widths of other complexes listed in Table IV are consistently larger by *ca.* 20% than in acetonitrile. An azomethine proton signal was detected only for $[Ni(PccBF)]^+$ and occurred at −207 ppm from TMS. The 6-H resonances of complexes **2**–**4** were not located and are undoubtedly severely broadened as is the 6,6′-H signal of $[Ni(bipy)_3]^{2+}$.[50] Aliphatic proton signals were not well resolved and not all were detected (*cf.* Figure 12). The spectrum of $[Ni(P(bipy)_3)]^{2+}$ is considered in a following section.

Because the Ni(II) complexes possess an orbital singlet ground state when $0 \leqslant \phi \leqslant 60°$, their isotropic shifts can be attributed predominantly to contact interactions, with little dipolar contribution. One basis for anticipating a correlation between twist angle and contact shifts of these complexes is that in TAP geometry the unpaired spin resides in d orbitals primarily involved in σ bonding, whereas in TP geometry the spin-containing d orbitals can mix with both ligand σ and π orbitals. The data in Table IV show that for complexes **1**–**4**, in which pyridine-2-carboxaldimine groups have sensibly constant orbital energies, shifts of $[Ni((py)_3tach)]^{2+}$ and $[Ni((py)_3tame)]^{2+}$ are comparable and are intermediate between those of $[Ni(PccBF)]^+$ and $[Ni((py)_3tren)]^{2+}$. If $[Ni(bipy)_3]^{2+}$ and $[Ni(P(py)_3)_2]^{2+}$ are included as limiting TAP cases no monotonic correlation exists. At the 4-position in particular, where π-spin density is indicated by downfield proton and upfield methyl shifts, there is no large variation in shifts for five of the six complexes. Only for $[Ni(PccBF)]^+$ does π-spin density at this position appear to be substantially increased. With the apparent exception of this complex, the insensitivity of contact shifts to stereochemistry may be attributed to the known tendency of pyridine-type ligands to delocalize primarily σ spin (ligand → metal spin transfer) even when unpaired spin exists in metal orbitals of π symmetry.[51] In the Co(II) series orbitally degenerate ground states are expected for all values of ϕ, such that sizable magnetic anisotropies and significant dipolar contributions to the isotropic shifts will occur.[52] Simultaneous variation of geometric factors[49] and anisotropies with twist angle renders unlikely any correlation of shifts with structure. No systematic trends in shifts (or line widths) have been found for the Co(II) complexes, and their pmr spectra are not considered further. Attention is directed to consideration of proton line widths δ of the series composed of the first five Ni(II) complexes in Table IV, whose spectra have been measured in acetonitrile.

Inspection of Table IV reveals some definite trends of δ for the three ring protons, especially for 3-H and 4-H, with structure. Line widths increase with increasing twist angle, being smallest for $[Ni(PccBF)]^+$ and largest for those species ($[Ni((py)_3tame)]^{2+}$, $[Ni(bipy)_3]^{2+}$, $[Ni(P(py)_3)_2]^{2+}$ (in DMSO)) which approach or perhaps achieve the TAP limit. Such trends in line width could serve as structural indicators if a model for a relationship between line widths and twist angles can be established.

Proton relaxation[53] in a stable paramagnetic complex can be described by eq 9[54] where $B = 7\gamma_H{}^2g^2\beta^2S\cdot(S+1)/15r^6$, $C = S(S+1)(A/\hbar)^2/3$, r is the proton–metal distance, and $A/\hbar$ is the proton hyperfine coupling constant (radians/sec).

$$\delta\pi = \frac{1}{T_2} = [B]\left[\tau_c + \frac{13\tau_c/7}{1 + \omega_s{}^2\tau_c{}^2}\right] + [C]\left[\tau_e + \frac{\tau_e}{1 + \omega_s{}^2\tau_e{}^2}\right] \qquad (9)$$

τ_c and τ_e are the correlation times for dipolar and hyperfine exchange relaxation, respectively. Other symbols have their usual meanings.[54] Correlation times are related by eq 10, where τ_s

$$\tau_c{}^{-1} = \tau_s{}^{-1} + \tau_r{}^{-1}, \quad \tau_e{}^{-1} = \tau_s{}^{-1} \qquad (10)$$

is the electron spin relaxation time and τ_r is the characteristic molecular tumbling time. Terms B and C can be calculated if r and $A/\hbar$ are known. The former is known or can be estimated from X-ray data and the latter is obtained from the observed contact shift by eq 11. The Curie dependence of shifts required by this

$$\frac{\Delta H}{H} = -\left(\frac{A}{h}\right)\frac{g\beta S(S+1)}{(\gamma_H/2\pi)3kT} \qquad (11)$$

equation has been verified for the Ni(II) complexes in the 0–77° range.

Previous analyses of line widths in Ni(II) complexes have dealt exclusively with octahedral species.[55] This analysis will focus on the origins of the decrease in δ as ϕ is *decreased* from *ca.* 60°. Using δ(4-H) of $[Ni(bipy)_3]^{2+}$, r(Ni–4-H) ~5.9 Å (*vide infra*), and the observed 4-H shift, it is estimated for this complex that $B/C \approx 36$ and $\tau_c \leqslant 3.5 \times 10^{-11}$ sec as a *lower* limit. An upper limit to τ_r is estimated from the Debye equation[56] as $\tau_r \geqslant 8 \times 10^{-9}$ sec. Similar values are obtained for $[Ni((py)_3tren)]^{2+}$. Hence, $\tau_c \ll \tau_r$ and, from eq 10, $\tau_c \cong \tau_s \cong \tau_e$. To compare line widths of these and other complexes in the series, values of r are required. X-Ray data for salts of $[Ni(PccBF)]^+$ and $[Ni((py)_3tach)]^{2+}$ [16] give Ni-4-C distances of *ca.* 4.8 Å, from which the above r(Ni-4-H) value was obtained. In $[Fe((py)_3tame)]^{2+}$,[19b] $[Zn((py)_3tame)]^{2+}$,[19a] and $[Ni(phen)_3]^{2+}$ (Table I) M-4-C distances calculated from atomic coordinates differ from those in the preceding two complexes primarily by the incremental differences in M–N distances. Values of r(Ni–4-H) in the series of complexes are therefore taken as 5.9 Å, which is considered the most reliably estimated Ni–H distance due to the near collinearity of Ni–N–4-C–4-H. With the constant r value and the range $36 \gtrsim (B/C) \gtrsim 7$ estimated for the series, the decrease in δ(4-H) with decreasing twist angle appears to reflect decreasing τ_c

---

[51] J. A. Happe and R. L. Ward *J. Chem. Phys.*, **39**, 1211 (1963); R. H. Holm, G. W. Everett, Jr., and W. D. Horrocks, Jr., *J. Amer. Chem. Soc.*, **88**, 1071 (1966); W. D. Horrocks, Jr., and D. L. Johnston, *Inorg. Chem.*, **10**, 1835 (1971).

[52] J. P. Jesson, *J. Chem. Phys.*, **47**, 582 (1967); W. D. Horrocks, Jr., *Inorg. Chem.*, **9**, 690 (1970).

[53] I. Solomon, *Phys. Rev.*, **99**, 559 (1955); N. Bloembergen, *J. Chem. Phys.*, **27**, 572 (1955).

[54] R. A. Bernheim, T. H. Brown, H. S. Gutowsky, and D. E. Woessner, *ibid.*, **30**, 950 (1959).

[55] N. Bloembergen and L. O. Morgan, *ibid.*, **34**, 842 (1961); W. B. Lewis and L. O. Morgan, *Transition Metal Chem.*, **4**, 33 (1968).

[56] $\tau_r = 4\pi\eta a^3/3kT$: $a \approx 6$ Å (molecular radius), η (viscosity) = 0.345 cP for acetonitrile.

at this position. Inasmuch as $\tau_c \cong \tau_s$ for the longest τ_c of $[\mathrm{Ni(bipy)_3}]^{2+}$ and $[\mathrm{Ni((py)_3tren)}]^{2+}$, decreasing δ also indicates decreasing τ_s.[57]

X-Ray results for $[\mathrm{Ni(PccBF)}]^+$, $[\mathrm{Ni((py)_3tach)}]^{2+}$, and $[\mathrm{(Fe,Zn)((py)_3tame)}]^{2+}$ indicate that M–3-C and M–5-C distances are nearly constant when corrected for ionic radius differences. The assumption that the corresponding Ni–H distances are approximately constant in the series appears justified. For 3-H and 5-H, $5 > (B/C) > 1$, so that both terms in eq 9 must be considered. Because of the nearly invariant ratio r(Ni–5-C)/r(Ni–3-C), the line width ratio δ(5-H)/δ(3-H) due to dipolar relaxation should be independent of complex. $A/\hbar$ for 3-H and 5-H is not a monotonic function of the twist angle, ϕ, with $(A/\hbar)_{3\text{-H}}$ slightly larger for small ϕ ($[\mathrm{Ni(PccBF)}]^+$) and $(A/\hbar)_{5\text{-H}}$ slightly larger for $\phi \approx 60°$ ($[\mathrm{Ni((py)_3tren)}]^{2+}$). Hence, the ratio δ(5-H)/δ(3-H) is expected to be relatively insensitive to ϕ, perhaps decreasing with decreasing ϕ, as long as a single $\tau_c \sim \tau_e \sim \tau_s$ is operative at all proton positions. Although δ(5-H)/δ(4-H) (range 4.1–5.1) is relatively insensitive to ϕ, δ(5-H)/δ(3-H) and δ(4-H)/δ(3-H) decrease about tenfold upon passing from $[\mathrm{Ni(PccBF)}]^+$ to $[\mathrm{Ni(bipy)_3}]^{2+}$, the order of increasing ϕ. This unusual behavior is considered below. Line widths at the three positions, however, are consistent in indicating decreasing τ_s as ϕ is decreased, even when terms in B and C are comparable.

Although the theory of electron spin relaxation is not completely understood in detail, the origin of relatively short τ_s values for Ni(II) in approximately octahedral coordination is generally attributed to modulation of the zero-field splitting (ZFS),[55] with $\tau_s \propto D^{-2}$. D is the ZFS parameter defined as the separation between the $S_z = \pm 1$ and 0 levels. Such splittings arise from the combined effects of spin–orbit coupling and an axial distortion.[58] In a trigonally distorted octahedron $D \propto (1/\Delta E_1 - 1/\Delta E_2) = (\Delta E_2 - \Delta E_1)/\Delta E_1 \Delta E_2$, where ΔE_1 and ΔE_2 correspond to the transitions $^3\mathrm{A_2(e_b{}^2)} \rightarrow {}^3\mathrm{A_1(e_b e_a)}$, $^3\mathrm{E(e_b a_1)}$, respectively. D is thus more sensitive to differences in ΔE_1 and ΔE_2 than to their exact magnitude. The orbital energies plotted in Figure 3 indicate that, within the one-electron approximation, $\Delta E_2 - \Delta E_1$ increases significantly with decreasing ϕ. D is therefore predicted to increase rapidly and τ_s to decrease as ϕ is decreased, providing a plausible explanation for changes in line widths with structure in a series of related complexes where similar molecular motions in solution[55,57] may be assumed. The argument is of course qualitative, for D also depends upon spin–orbit interactions[58] whose matrix elements are functions of ϕ. However, the (estimated) sizable variations in $\Delta E_2 - \Delta E_1$ are expected to dominate changes in D upon passing from the TAP to the TP configuration.

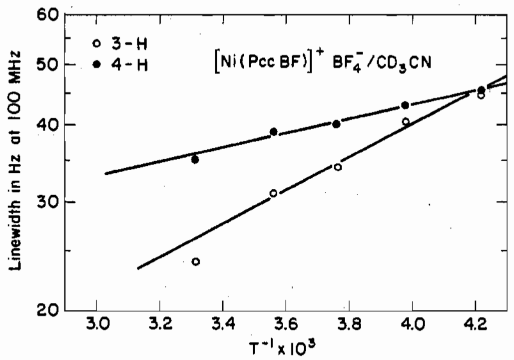

Figure 13.—Plot of log (line width) *vs.* $1/T$ for 3-H and 4-H signals of $[\mathrm{Ni(PccBF)}]^+$ in $\mathrm{CD_3CN}$.

Since $\tau_c \sim \tau_e \sim \tau_s$, use of eq 9 involves the assumption that a single τ_s is operative at all proton positions in a given molecule, such that the relative line widths for different protons are given by the relative values of B and/or C. The values for r discussed above and the $A/\hbar$ data obtained from the contact shifts dictate that the relative line widths should follow the order δ(4-H)/δ(3-H) < 1, δ(5-H)/δ(3-H) $\lesssim 1$, and δ(5-H)/δ(4-H) > 1. These relationships are satisfied simultaneously only by $[\mathrm{Ni(bipy)_3}]^{2+}$ and $[\mathrm{Ni((py)_3tren)}]^{2+}$.[59] As the twist angle is decreased ratios involving δ(3-H) show increasing deviation from expected values; *e.g.*, δ(5-H)/δ(3-H) increases from 0.71 for $[\mathrm{Ni(bipy)_3}]^{2+}$ to 7.5 for $[\mathrm{Ni(PccBF)}]^+$. As noted above δ(5-H)/δ(4-H) is nearly invariant throughout the series. This behavior can be rationalized by assuming the existence of two correlation times: τ_s, operative at both 4-H and 5-H, and $\tau^* < \tau_s$, operative primarily at 3-H in complexes with $\phi <$ 50–60°. Thus the change in δ(5-H)/δ(3-H) indicates that τ^* decreases with ϕ but at a faster rate than τ_s. Experimental evidence for the existence of different τ_c's at 3-H and 4-H can be obtained from the temperature dependencies of the line widths. Since τ_c may be expressed[54] as $\tau_c = \tau_c{}^\circ \exp(V/RT)$, a plot of log δ *vs.* T^{-1} should yield a series of parallel lines with slope V/R for a given complex with a single correlation time, as observed for the related complex $[\mathrm{Cr(phen)_3}]^{2+}$.[60] A plot of this type for $[\mathrm{Ni(PccBF)}]^+$, illustrated in Figure 13, shows that different τ_c's are operative. The exact nature[61] of the local correlation time τ^* is not understood, and more extensive studies of the temperature and magnetic field dependence of line widths will be required to characterize this novel relaxation phenomenon.

Polarography.—In order to determine whether redox properties were sensitive to structural variation, the polarographic behavior of the complexes **1**–**4** and **7** in acetonitrile solution have been investigated. Half-wave potentials for one-electron redox reactions observed in the range −2.0 to +2.0 V *vs.* sce are collected in Table V. These reactions were not strictly reversible electrochemically in the majority of cases, as judged from the slopes ($|E_{3/4} - E_{1/4}|$) of current–voltage curves,

---

[57] That line width trends are dominated by electronic effects associated with structural differences and not by changes in τ_r is further supported by the large disparities in δ between $[\mathrm{Ni(bipy)_3}]^{2+}$ and $[\mathrm{Ni(P(bipy)_3)}]^{2+}$ (Table IV), which should have quite similar mean radii.

[58] C. J. Ballhausen, "Introduction to Ligand Field Theory," McGraw-Hill, New York, N. Y., 1962, pp 134–135.

[59] More exact comparisons of predicted and observed line width ratios cannot be made at present due to the lack of accurate Ni–H distances.

[60] G. N. LaMar and G. R. Van Hecke, *J. Chem. Phys.*, **52**, 5676 (1970).

[61] Because the effect of τ^* appears to be localized primarily at the 3-H position, near the azomethine–pyridyl junction, it is tentatively suggested that this correlation time may be associated with vibrations arising from distortions within a ligand. The structure of $[\mathrm{Fe(PccBF)}](\mathrm{BF_4})$[9b] indicates that this junction is a point of flexibility inasmuch as the complex achieves a non-TP structure in part by twisting the azomethine and pyridyl groups out of a coplanar arrangement. Data for non-TAP complexes (Table I) reveal the lack of a strict C_3 axis with one twist angle different from the other two. In solution the distortions producing this effect would not be expected to be confined to a unique ligand but would "pseudorotate" among the three chelate rings. It is likely that the importance of strain and associated vibrations upon correlation times decreases with the less constrained complexes, *i.e.*, as TAP geometry is approached.

TABLE V

HALF-WAVE POTENTIALS FOR TRIGONAL M–N_6 COMPLEXES IN ACETONITRILE AT 25°

	$E_{1/2}$,[a] V		
Complex	$(z-2) \rightarrow (z-1)$	$(z-1) \rightarrow z$	$z \rightarrow (z+1)$
$[Fe(PccBF)]^+$	−1.52	−0.41	+1.24[b]
$[Fe((py)_3tach)]^{2+}$	−1.37	−1.03	+1.16[b]
$[Fe((py)_3tame)]^{2+}$	−1.51	−1.24	+1.2[b]
$[Fe((py)_3tren)]^{2+}$	−1.52	−1.17	+0.93[b]
$[Fe(P(CH_3pox)_3)]^{2+}$	−2.0	−0.93	∼+1.5[b,e]
$[Fe(P(bipy)_3)]^{2+}$	−1.32	−0.96	+1.16[b]
$[Co(PccBF)]^+$	−1.70	−0.29[c]	≳+1.2[d,e]
$[Co((py)_3tach)]^{2+}$	−1.54	−0.66[c]	+0.47[d]
$[Co((py)_3tame)]^{2+}$	−1.53	−0.68[c]	+0.17[d]
$[Co((py)_3tren)]^{2+}$	*g*	−0.99[c]	+0.48[d]
$[Co(P(CH_3pox)_3)]^{2+}$	*g*	−0.37[c]	≳+1.1[d,e]
$[Co(P(bipy)_3)]^{2+}$	*g*	−0.66[c]	≳+0.8[d,e]
$[Co(P(py)_3)_2]^{2+}$	*g*	−0.92[c]	+0.55[d]
$[Co(bipy)_3]^{2+}$	*g*	−0.95[c]	+0.32[d]
$[Ni(PccBF)]^+$	−1.62	−0.81	*f*
$[Zn(PccBF)]^+$	−1.54	−1.17	*f*

[a] Measured at rpe, *vs.* sce; charge z given in first column. The calibrant for diffusion currents corresponding to one-electron transfer was $[Cr(S_2C_2(CN)_2)_3]^{3-}$ (A. Davison, N. Edelstein, R. H. Holm, and A. H. Maki, *J. Amer. Chem. Soc.*, **86**, 2799 (1964)). [b] Fe(II) → Fe(III). [c] Co(I) → Co(II). [d] Co(II) → Co(III). [e] Poorly defined wave. [f] Oxidation not observed. [g] Apparent n-electron reduction ($n \geq 2$) in the range −1.5 to −1.8 V.

which usually exceeded the theoretical value of 56 mV. However, the data do serve to define the redox patterns of the various complexes within the stated potential interval.

The complexes in Table V usually exhibit two reduction steps and a single oxidation. The second reduction occurs in the range of *ca.* −1.4 to −1.7 V and presumably corresponds to addition of an electron to the ligand system. The first reduction of $[Zn(PccBF)]^+$ is interpreted similarly. This complex also displays a third, less well-defined reduction at −2.0 V. As indicated in the table, oxidation of the Fe(II) and Co(II) complexes is interpreted as M(II) → M(III) and the first reduction of the latter as Co(II) → Co(I).[62] Of these processes only the reductions closely approach reversibility, with slopes not exceeding 70 mV. Half-wave potentials for the first reductions exhibit a marked dependence on stereochemistry in the Co(II) series. As measured by $E_{1/2}$ values electron affinity is highest for $[Co(PccBF)]^+$ and lowest for $[Co((py)_3tren)]^{2+}$, $[Co(P(py)_3)_2]^{2+}$, and $[Co(bipy)_3]^{2+}$. The potentials span a range of 0.70 V and differ only slightly among the latter three complexes, which are near the TAP limit. The potentials also indicate that $[Co(PccBF)]^+$ is more difficult to oxidize than the other Co(II) species and that $[Fe(PccBF)]^+$ is more readily reduced than other members of the Fe(II) series **1**–**4**. It is observed that the relative ease of reduction of $[Co(PccBF)]^+$ may account for the persistence of small amounts of the Co(I) complex in samples of this compound and that the high positive oxidation potential of $[Fe((py)_3tame)]^{2+}$ may be responsible for the claimed inertness of its analog to oxidation by Ce(IV).[18]

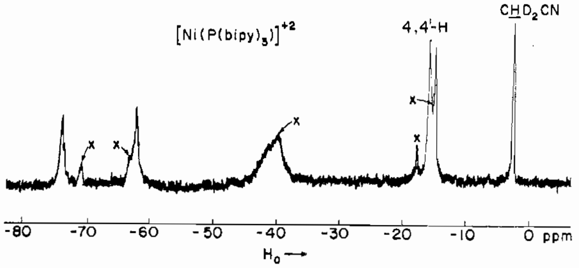

Figure 14. Pmr spectrum (100 MHz) of $[Ni(P(bipy)_3)](ClO_4)_2$ (**6**) in CD_3CN at ∼29°. 3,3′-H and 5,5′-H signals are tentatively assigned in Table IV. Impurity signals are indicated by an ×. Only the sharp spike in the resonance at *ca.* −40 ppm is due to an impurity.

Stereochemistry of $[M(P(CH_3pox)_3)]^{2+}$ and $[M(P(bipy)_3)]^{2+}$.—The trends in ligand-field transition energies, pmr line widths, and polarographic half-wave potentials with twist angle for certain complexes in the series **1**–**4**, **7**, and $[M(bipy)_3]^{2+}$ offer the possibility of empirical deduction of the approximate stereochemistry (in terms of ϕ) of other complexes of the basic tris(α-diimine) type. For this purpose the new sexadentate complexes $[M(P(CH_3pox)_3)]^{2+}$ (**5**) and $[M(P(bipy)_3)]^{2+}$ (**6**) (Figure 1), M = Fe(II), Co(II), Ni(II), have been synthesized. No X-ray structural data are available for these species. Complexes **5** and **6** have as closest analogs in terms of ligand structure **1** and $[M(bipy)_3]^{2+}$, respectively, and resemble the sexadentates **2**–**4** by virtue of their open trifurcated structure. They therefore lack the high degree of structural rigidity of $[M(PccBF)]^+$ complexes, and space-filling molecular models suggest that **5** and **6** can approach both the TP and TAP configurations.

Considering first the Ni(II) complexes, ligand-field spectral information for $[Ni(P(CH_3pox)_3)]^{2+}$ and $[Ni(P(bipy)_3)]^{2+}$ are given in Table III and Figure 8. For reasons discussed above, the features at 11,700 and 11,900 cm^{-1} are assigned as spin-forbidden bands. The transitions at 10,500 (ϵ 17) and 10,700 cm^{-1} (ϵ 20) are assigned to triplet–triplet transitions and are intermediate in energy between $[Ni(PccBF)]^+$ and $[Ni((py)_3tach)]^{2+}$. Intensities of these features are considerably larger than those of complexes near the TAP limit. Pmr data for $[Ni(P(bipy)_3)]^{2+}$ are given in Table IV, and the spectrum at ambient temperature is shown in Figure 14. The complex contains two inequivalent types of pyridyl rings, accounting for the two pairs of signals centered at *ca.* −15 and −68 ppm. The feature at *ca.* −40 ppm was not clearly resolved into two resonances. Signal assignments were made by analogy with isotropic shifts and line widths of other complexes in Table IV. Assignment of the 4,4′-H resonances is the most reliable since these features have the smallest shifts and, except for $[Ni(PccBF)]^+$, the narrowest line widths in all complexes. Assuming Ni–3-H, -4-H, and -5-H distances similar to those of other complexes and using the observed isotropic shifts, it is found that B/C values for protons on the ring bonded to phosphorus fall into the ranges specified above. Hence, the line widths, especially δ(4-H), and line width ratios suggest a structure which deviates considerably from the TP and TAP limits. In particular, the line width ratios suggest the existence of two correlation times, a feature associated with non-TAP

---

(62) The first reduction of $[Co(bipy)_3]^{2+}$ has been amply demonstrated to yield $[Co^I(bipy)_3]^+$.[48,63] For a more detailed electrochemical study *cf.* ref 63c.

(63) (a) B. Martin, W. R. McWhinnie, and G. M. Waind, *J. Inorg. Nucl. Chem.*, **23**, 207 (1961); (b) R. J. Fitzgerald, B. B. Hutchinson, and K. Nakamoto, *Inorg. Chem.*, **9**, 2618 (1970); (c) N. Tanaka and Y. Sato, *Bull. Chem. Soc. Jap.*, **41**, 2059 (1968), and references therein.

complexes. Both the line widths and their ratios imply a stereochemistry comparable to $[Ni((py)_3tach)]^{2+}$. Therefore, it is concluded that $[Ni(P(bipy)_3)]^{2+}$ possesses an intermediate solution stereochemistry with ϕ perhaps near *ca.* 30°. A similar structure is proposed for $[Ni(P(CH_3pox)_3)]^{2+}$ on the basis of spectral data only. Attempts to measure pmr spectra in solvents in which the salt of the complex was sufficiently soluble resulted in partial solvation of the nickel ion, and suitable spectra of the intact complex could not be obtained.

Ligand-field spectral data for $[Co(P(CH_3pox)_3)]^{2+}$ and $[Co(P(bipy)_3)]^{2+}$ (Table III and Figure 9) reveal that the near-infrared ligand-field bands of these complexes occur at energies intermediate between those of TP and TAP species and most nearly coincide with that of $[Co((py)_3tach)]^{2+}$. Half-wave potentials for the nearly reversible Co(II) → Co(I) reductions of these two complexes are considerably less cathodic than those in the narrow range (−0.92 to −0.99 V) associated with complexes having $\phi \geq 49°$. The potential for the $P(bipy)_3$ species is essentially identical with those of $[Co((py)_3tach)]^{2+}$ and $[Co((py)_3tame)]^{2+}$, whereas that of $[Co(P(CH_3pox)_3)]^{2+}$ is within 10 mV of $[Co(PccBF)]^+$. The spectral and polarographic results suggest that solution stereochemistry of the two Co(II) complexes is comparable to that of the $(py)_3tach$ or $(py)_3tame$ species, with that of $[Co(P(CH_3pox)_3)]^{2+}$ perhaps the more displaced toward the TP limit. The lack of accurate structural data for $[Co((py)_3tach)]^{2+}$ and $[Co((py)_3tame)]^{2+}$ (*cf.* Table I) and the possible structural difference of the former in the solid and solution phases, noted above, preclude a further assessment.

Investigation of spectral and nmr properties of the Fe(II) complexes **1**–**4** and **7** has failed to reveal any systematic trends with stereochemistry. The polarographic data (Table V) indicate that the first reduction potentials for complexes **2**–**4** show only a moderate variation but occur at potentials *ca.* 0.6 V or more cathodic than that of $[Fe(PccBF)]^+$, which has the smallest average twist angle of any Fe(II) complex. Reduction potentials of $[Fe(P(CH_3pox)_3)]^{2+}$ and $[Fe(P(bipy)_3)]^{2+}$ are clearly near those of complexes with twist angles in excess of *ca.* 40°. A potentially more sensitive structural probe is the quadrupole splitting of the iron nucleus measured by Mössbauer spectroscopy. Recent measurements by Reiff[64] have yielded the following values of ΔE_Q (mm/sec): $[Fe(PccBF)]^+$, 0.95; $[Fe((py)_3tame)]^{2+}$, 0.41; $[Fe((py)_3tren)]^{2+}$, 0.38; $[Fe((py)_3tach)]^{2+}$, 0.29; $[Fe(P(py)_3)_2]^{2+}$, 0. The series as written indicates, approximately, decreasing departure from effective octahedral symmetry. The values for $[Fe(P(CH_3pox)_3)]^{2+}$ and $[Fe(P(bipy)_3)]^{2+}$, 0.20 and ~0 mm/sec, respectively, suggest solid-state structures approaching the TAP limit. A detailed analysis of the Mössbauer spectra will be presented subsequently.[64]

These results suggest that the Co(II), Ni(II), and Fe(II) complexes **5** and **6** follow series 4 and that, for a given metal ion, $P(CH_3pox)_3$ may have a slightly greater tendency than $P(bipy)_3$ to stabilize geometries nearer to the TP limit.

Acknowledgments.—This research was supported by the National Science Foundation and the National Institutes of Health under Grants GP-18978X and GM-15471, respectively. We thank Drs. M. R. Churchill, Q. Fernando, E. B. Fleischer, E. C. Lingafelter, A. H. Reis, Jr., W. M. Reiff, N. J. Rose, D. Templeton, and A. Zalkin for disclosure of results prior to publication and for permission to quote certain of these results. Several useful discussions with A. H. Reis, Jr., are acknowledged.

Appendix

The angular overlap model[33,36] has been applied to the calculation of orbital energies and energy levels for d^7 and d^8 systems of D_{3h} and D_3 symmetry. Using the coordinate system of Figure 2 and eq 5, general expressions for the orbital energies are

$$E(e'') = \sum_{i=1}^{6}\left[\left(\frac{\sqrt{3}}{2}\sin 2\theta_i \cos \phi_i\right)^2 e_\sigma + (-\sin \phi_i \cos \theta_i \cos \psi_i - \cos \phi_i \cos 2\theta_i \sin \psi_i)^2 e_{\pi^s} + (-\sin \phi_i \cos \theta_i \sin \psi_i + \cos \phi_i \cos 2\theta_i \cos \psi_i)^2 e_{\pi^c}\right] \quad (12)$$

$$E(e') = \sum_{i=1}^{6}\left[\left(\frac{\sqrt{3}}{2}\sin^2 \theta_i \sin 2\phi_i\right)^2 e_\sigma + \left(\cos 2\phi_i \sin \theta_i \cos \psi_i - \frac{1}{2}\sin 2\phi_i \sin 2\theta_i \sin \psi_i\right)^2 e_{\pi^s} + \left(\cos 2\phi_i \sin \theta_i \sin \psi_i + \frac{1}{2}\sin 2\phi_i \sin 2\theta_i \cos \psi_i\right)^2 e_{\pi^c}\right] \quad (13)$$

$$E(a_1') = \sum_{i=1}^{6}\left[\left(\frac{1}{4} + \frac{3}{4}\cos 2\theta_i\right)^2 e_\sigma + \left(\frac{\sqrt{3}}{2}\sin 2\theta_i \sin \psi_i\right)^2 e_\pi + \left(\frac{\sqrt{3}}{2}\sin 2\theta_i \cos \psi_i\right)^2 e_{\pi^c}\right] \quad (14)$$

When $\phi > 0°$, $e'' \rightarrow e_b$, $e' \rightarrow e_a$, and $a_1' \rightarrow a_1$ (Figure 3). The parameter e_σ has its usual meaning and e_{π^s} and e_{π^c} represent the (anti)bonding effects of the ligand out-of-plane and in-plane orbitals, respectively, having π character with respect to the metal–ligand bond. The magnitudes of these parameters are usually considered[36] to fall in the order $e_\sigma > |e_{\pi^s}| \gtrsim |e_{\pi^c}|$. In complexes **1**–**7** the π^c orbitals are heavily involved in ligand σ-framework bonding and their interaction with metal d orbitals should be slight. Taking $\alpha = 77°$ from the structure of $[Ni(PccBF)](BF_4)$[9a] and $\theta = 51.5°$ in the TP limit, the following orbital energies are obtained.

$$E(e'') = 2.136e_\sigma + 1.163e_{\pi^s} + 0.152e_{\pi^c}$$
$$E(e') = 0.844e_\sigma + 1.837e_{\pi^s} + 0.712e_{\pi^c}$$
$$E(a_1') = 0.004e_\sigma + 4.272e_{\pi^c}$$

Reasonable limits for the ratio Δ_1/Δ_2 can be gauged by assuming $e_{\pi^c} = 0$ and $e_{\pi^s} = \pm 0.1e_\sigma$, which are considered limiting values for e_{π^s}. The following ratios are readily obtained: 0.84 ($e_{\pi^s} = +0.1e_\sigma$), 0.48 ($e_{\pi^s} = -0.1e_\sigma$), 0.65 ($e_{\pi^s} = 0$).

Employing standard procedures the secular determinants for all triplet states from the ^3F and ^3P free ion terms and the only relevant singlet state (from ^1D)

---

[64] W. M. Reiff, results to be published.

were obtained for d^8 and solved. Determinants for the quartet d^7 states are obtained by reversing the signs of all diagonal elements in the triplet determinants. Energy-level diagrams for d^7 and d^8 with different Δ_1/Δ_2 values have been constructed using Δ_2/B as a variable and $C = 4B$. Diagrams of this type are shown in Figure 10. Calculations were also performed for the d^8 case with $0° \leqslant \theta \leqslant 60°$ using a constant α value of 77° inasmuch as the available structural data (Table I) do not indicate a large variation of this angle with ϕ. A procedure similar to that for the $\phi = 0°$ case was used with appropriate values of angular coordinates in eq 12–14. Calculations were carried out with $e_\sigma = 3B–6B$, $e_{\pi^s} = e_{\pi^c} = 0$, and with $e_\sigma = 4B$, $e_{\pi^s} = 0.2e_\sigma$, $e_{\pi^c} = 0$; in all cases $C = 4B$. One such energy-level diagram is given in Figure 11 and illustrates the usual order of triplet states for a given ϕ over the range of parameterization.

CONTRIBUTION FROM THE DEPARTMENT OF CHEMISTRY,
MASSACHUSETTS INSTITUTE OF TECHNOLOGY, CAMBRIDGE, MASSACHUSETTS 02139

Enumeration of Permutational Isomerization Reactions. II[1]

BY W. G. KLEMPERER[2]

Received April 13, 1972

In a previous paper, classes of symmetry equivalent permutational isomerization reactions were defined and exhaustively enumerated for symmetric molecules with identical substituents.[1] In the present paper this treatment is extended to molecules whose substituents are not necessarily identical. The generalized treatment is used to enumerate all distinct permutational isomerization reactions of molecules MH_nP_4, $n = 1, 2, 3,$ or 4, where M is a transition metal, H is a hydride ligand, and P is a trisubstituted phosphorus ligand. The importance of these results for the interpretation of temperature-dependent nmr line-shape behavior is stressed.

I. Introduction

It will be assumed throughout this paper that the reader is familiar with the author's paper, "Enumeration of Permutational Isomerization Reactions"[1] (EPIR-I). In EPIR-I, classes of symmetry equivalent permutational isomerization reactions are defined, assuming that all ligands which are permuted are identical. All permutational isomers of a given molecule must have in common the same molecular skeleton. If all the ligands are not identical, then the permutation of two nonidentical ligands may lead to a change in molecular geometry and therefore a change in the molecular skeleton. Such a permutation would not define a permutational isomerization reaction. In the case of molecules of the type MH_nP_4 (see Figure 1), the P ligands and H ligands are clearly not identical and the methods of EPIR-I become chemically meaningless.

In the following section, the concepts defined in EPIR-I will be generalized to allow enumeration of the permutational isomerization reactions of molecules with sets of nonidentical ligands. These concepts will then be used to treat molecules of the type MH_nP_4.

II. Generalized Definitions

A. The Group of Allowed Permutations.—As in EPIR-I, permutational isomers[3] are defined as "chemical compounds which have in common the same molecular skeleton and set of ligands, differing only by the distribution of ligands on the skeletal positions." The set of indexed unidentate ligand labels $\mathbf{L}_l = \{l_1, l_2, \ldots, l_n\}$ and the set of indexed skeletal position labels $\chi_s = \{s_1, s_2, \ldots, s_n\}$ are combined to form a $2 \times n$ matrix $\binom{l}{s}$. Thus

$$\begin{pmatrix} l \\ s \end{pmatrix} = \begin{pmatrix} 12\ldots n \\ ij\ldots k \end{pmatrix}$$

lists the ligand indices in the top row and below each ligand index is placed the index of the skeletal position which that ligand occupies. A permutational isomerization reaction is described by a permutation p_i which acts on the indices of the skeletal positions. The set of all permutations which describe permutational isomerization reactions and/or point group operations forms a group called the *group of allowed permutations*.

In EPIR-I it is assumed that all n ligands are identical and therefore any one of the $n!$ permutations in the symmetric group S_n is an allowed permutation. If all n ligands are not identical, then some elements in S_n do not represent permutational isomerization reactions and the group of allowed permutations must be a subgroup of S_n. Consider, for example, the isomers shown in Figure 2. The permutation $p_i = (1)(2)(3)(4)(56)$ will convert isomer a into isomer b if skeletal positions are indexed as in Figure 1. Since a and b are permutational isomers, p_i represents a permutational isomerization reaction; *i.e.*, p_i is an allowed permutation. The permutation $q_i = (1)(25)(3)(4)(6)$ converts isomer a into isomer c. Since a and c are polytopal isomers[4] but not permutational isomers, q_i does not represent a permutational isomerization reaction; *i.e.*, q_i is not an allowed permutation. As defined above, permutational isomers must have in common the same molecular skeleton. Isomers a and c clearly do not: a has a C_{2v} molecular skeleton, while c has a D_{4h} molecular skeleton.

---

[1] Part I: W. G. Klemperer, *J. Chem. Phys.*, **56**, 5478 (1972).

[2] National Science Foundation Predoctoral Fellow. Present address: Department of Chemistry, Texas A & M University, College Station, Texas 77843.

[3] I. Ugi, D. Marquarding, H. Klusacek, G. Gokel, and P. Gillespie, *Angew. Chem.*, **82**, 741 (1970); *Angew. Chem., Int. Ed. Engl.*, **9**, 703 (1970).

[4] E. L. Muetterties, *J. Amer. Chem. Soc.*, **91**, 1636 (1969).